This document is the unedited Author's version of a Submitted Work that was subsequently accepted for publication in Industrial & Engineering Chemistry Research, copyright © American Chemical Society after peer review. To access the final edited and published version see DOI: 10.1021/acs.iecr.0c00840

Nitroxide Mediated Miniemulsion Polymerization of Bio-based Methacrylates

*Saeid Tajbakhsh, Faezeh Hajiali and Milan Marić **

Department of Chemical Engineering, McGill University, 3610 University St. Montreal, H3A 0C5 Quebec, Canada.

KEYWORDS

Miniemulsion polymerization, Sustainability, Bio-sourced monomers, Methacrylates, Nitroxide-mediated polymerization.

ABSTRACT

Nitroxide-mediated homo and statistical copolymerization of commercially available methacrylates derived from sustainable feedstocks (isobornyl methacrylate (IBOMA) and a mixture of methacrylic esters with average alkyl side chain length = 13 units (termed C13MA)) was conducted in organic solvent (toluene) and in dispersed aqueous media using an oil-soluble unimolecular initiator (Dispolreg 007) without any controlling comonomers in a controlled manner. IBOMA homopolymerization in emulsion at 83-100 °C revealed the optimal polymerization temperature of 90 °C giving relatively narrow molecular weight distributions

(1.46< dispersities ($Đ$) <1.58) and conversion up to 83% in relatively short time (2 hours). IBOMA/C13MA statistical copolymerizations yielded copolymers with tunable glass transition temperature ($\mathrm{T_g}$) prepared in emulsion (-52 °C < $\mathrm{T_g}$ <123 °C) and in organic solvent (-40 °C < $\mathrm{T_g}$ < 169 °C). Resins made in emulsion at 90 °C proceeded up to 92.7% conversion with monomodal molecular weight distributions ($\overline{M}_n$ up to 68000 g mol^{-1} and $Đ$ = 1.62 - 1.72) and were colloidally stable (24% solids and final average particle sizes = 270-481 nm). Furthermore, chain end fidelity was verified by chain extensions with IBOMA and C13MA monomers in both emulsion and organic solvent. These results constitute a readily scalable route to make polymers via nitroxide mediated polymerization with controlled architecture using bio-based feedstocks without the hazards of bulk or homogeneous organic solvent polymerization.

INTRODUCTION

During the last couple of decades, there has been a high demand for developing industrially scalable polymerization processes to obtain materials with specific properties using controlled radical polymerization[1-3]. A controlled polymerization is considered akin to a living polymerization, which forms well-defined microstructures and produces polymers with narrow molecular weight distribution, displays a linear degree of polymerization versus conversion and active chain ends[4, 5]. To answer the demand for robust polymerization processes while controlling microstructure, reversible deactivation radical polymerization (RDRP), sometimes known as controlled radical polymerization (CRP), like nitroxide-mediated polymerization (NMP)[6, 7], reversible addition-fragmentation chain transfer (RAFT) polymerization[8, 9] and atom transfer radical polymerization (ATRP)[3, 10, 11] has been offered as one possibility. The main characteristics of all CRP methods include relatively narrow molecular weight distribution and active polymer chain ends[12], traits typically exhibited by truly living polymerizations. Unlike living polymerizations, CRP can be readily done in dispersed aqueous media [6, 13-15]. In particular, NMP possesses some distinctive attractive features. For example, NMP often simply relies on an alkoxyamine and heat to start a polymerization. Unlike traditional RAFT and ATRP, it does not suffer from discoloration issues or unpleasant odor from any metallic ligands or sulfur-based chain transfer agents, thereby eschewing exhaustive post-polymerization treatments to remove residual catalysts or other reagents[13, 16]. It should be noted that the advent of single electron transfer-living radical polymerization (SET-LRP), activators regenerated by electron transfer (ARGET ATRP), non-metal ATRP methods and novel RAFT agents have been reported to address discoloration and odor issues [7, 12, 17-27]. At first, NMP was very limited, restricted to the synthesis of styrenic-based polymers[28]. However, NMP was improved dramatically due to the development of new alkoxyamines. Benoit *et al.*[29, 30] developed alkoxyamines based on 2,2,5-tri-methyl-4-phenyl-3-azahexane-3-nitroxide (TIPNO), which can be used for the controlled polymerization of a wide range of monomers at lower temperatures. Further improvement occurred by the introduction of N-tert-butyl-N-[1-diethylphosphono-(2,2-dimethylpropyl)] (SG1) nitroxide. A commercially available SG1-based alkoxyamine, N-(2-methylpropyl)-N-(1-(diethylphosphono-2,2-dimethylpropyl)-O-(2-carboxylprop-2 yl)hydroxylamine) BlocBuilder-MA™ (termed herein as BB, from Arkema) has enabled homopolymerization of acrylates and acrylamides and under certain conditions, methacrylates (Figure 1(a) shows the chemical structure of BB) [6, 31, 32]. The polymerization of methacrylates using BB is problematic because of the high activation/deactivation equilibrium constant (K) of methacrylates and the cross-disproportionation effect [33-35]. To overcome this, the copolymerization method first described by Charleux and coworkers[36] was applied, where methacrylates are copolymerized with a small amount of comonomer with a very low K such as styrene[34, 37], acrylonitrile (AN)[38, 39], 9-(4-vinylbenzyl)-9H-carbazole[40, 41] or other styrenic derivatives[42-44]. As a result, the average K, $\langle K \rangle$, of the polymerization decreases and control is enhanced, accordingly[34]. Synthesizing an alkoxyamine applicable for a wide range of monomers, with low dispersity, low reaction temperature and active chain ends has always been challenging[45-47]. Recently, Ballard *et al.* [48, 49] reported a new group of alkoxyamines such as 3-(((2-cyanopropan-2-yl) oxy) - (cyclohexyl) amino)-2, 2-dimethyl-3-phenylpropanenitrile (Dispolreg 007), that enabled homopolymerization of methacrylates without any comonomer at temperatures < 100 ºC and allowed clean cross-over from a methacrylic block to a styrenic block. These conditions also enabled clean homopolymerization of methacrylates in emulsion or suspension media[48, 50]. This initiator is used in our study to control the polymerization. Figure 1(b) depicts the chemical formula of the Dispolreg 007 alkoxyamine.

Polymerization in dispersed aqueous media has advantages over solution or bulk polymerization methods. Bulk polymerization often results in highly viscous mixtures with attendant autoacceleration effects [28]. Solution polymerizations decrease viscosity but introduce issues regarding the removal of solvent. Using water as the continuous phase decreases the viscosity of the solution and improves heat transfer effects [51]. Further, such emulsions do not possess volatile organic compounds (VOC) which makes them a perfect choice for many indoor applications[52, 53]. NMP of methacrylates has been done in suspension[54], emulsion[55-57], miniemulsion [58-60] and microemulsion[61, 62]. These variants all have merits and detractions. Suspension polymerization is simple to implement industrially but its possible lack of colloidal stability, high tendency for agglomeration and low compartmentalization of nitroxide and radicals may pose problems towards obtaining resins with desirable properties [63-65]. In emulsion systems, partitioning of reactants reduces the control over the polymerization. In addition, microemulsion polymerization requires high surfactant concentrations and very high shear treatments and usually low monomer content (in the range of 1~10 wt%) which directly affects the polymer structure and reduces its applicability [28, 61, 66-68]. Miniemulsion techniques have been cited with many advantages[69-71]. Reactions in miniemulsions occur inside monomer droplets (50~1000 nm) where transportation of monomers is not an issue and compartmentalization effects allow very high conversion while maintaining low dispersity, viscosity and high colloidal stability[13, 72-76].

Shunning organic solvent in favour of water is one example of applying the principles of green chemistry; using sustainably-sourced monomers in place of petro-based ones is another key component, which is the additional focus of this work [77-79]. In organic solvents, NMP, RAFT and ATRP methods have been used with bio-based monomers [80-86]. Recently, Noppalit *et al.*[87] studied the nitroxide-mediated miniemulsion polymerization of bio-based tetrahydrogeraniol methacrylate and cyclademol methacrylate using Dispolreg 007. In the present study, NMP of commercially available bio-based isobornyl methacrylate (Terra Visiomer IBOMA from Evonik) and C13 methacrylate (methacrylic ester 13.0, C13MA, from Evonik) was conducted in organic solvent and then in emulsion. IBOMA is derived from pine sap (produced by the reaction of camphene and methacrylic acid; the camphene was made by isomerization of terpenes derived from pine sap[88]) and contains a bulky bicyclic group to afford high thermal stability [89, 90] resulting in a high glass transition temperature ($T_g \approx 110{\sim}200$ °C)[91-94] and can be copolymerized with other monomers to improve heat resistance [83, 95, 96]. C13MA is obtained from plant oils and provides flexibility to resins due to its long aliphatic side-chain [97]. The low T_g of poly(C13MA) (-46 °C) is attractive for copolymerization with other monomers to impart flexibility to coatings and thermoplastic elastomers, for example [91, 98-101]. RDRP in emulsion of bio-based monomers was reported via RAFT, in which Genggeng *et al.*[102] studied the RAFT emulsion polymerization of renewablysourced γ-methyl-α-methylene-γ-butyrolactone monomers. We also attempted to minimize or eliminate catalysts, agents, organic solvents and purification steps while maintaining the control of the polymerization and ultimately properties. In addition, moderate reaction temperature was applied for the initiation and polymerization which reduces the energy consumption. In the succeeding sections, we aim to translate the NMP of IBOMA and C13MA into a process in dispersed aqueous media with the requisite ability to make statistical and block copolymers. The reaction scheme of IBOMA and C13MA initiated by Dispolreg 007 is summarized in Figure 2.

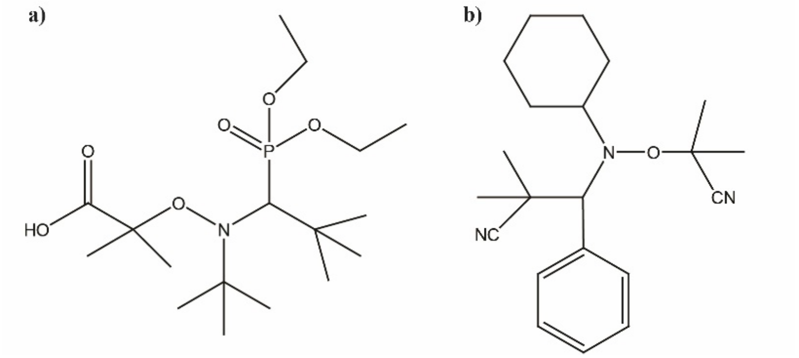

Figure 1. Chemical structures of (a) BlocBuilder™ (b) Dispolreg 007 alkoxyamines.

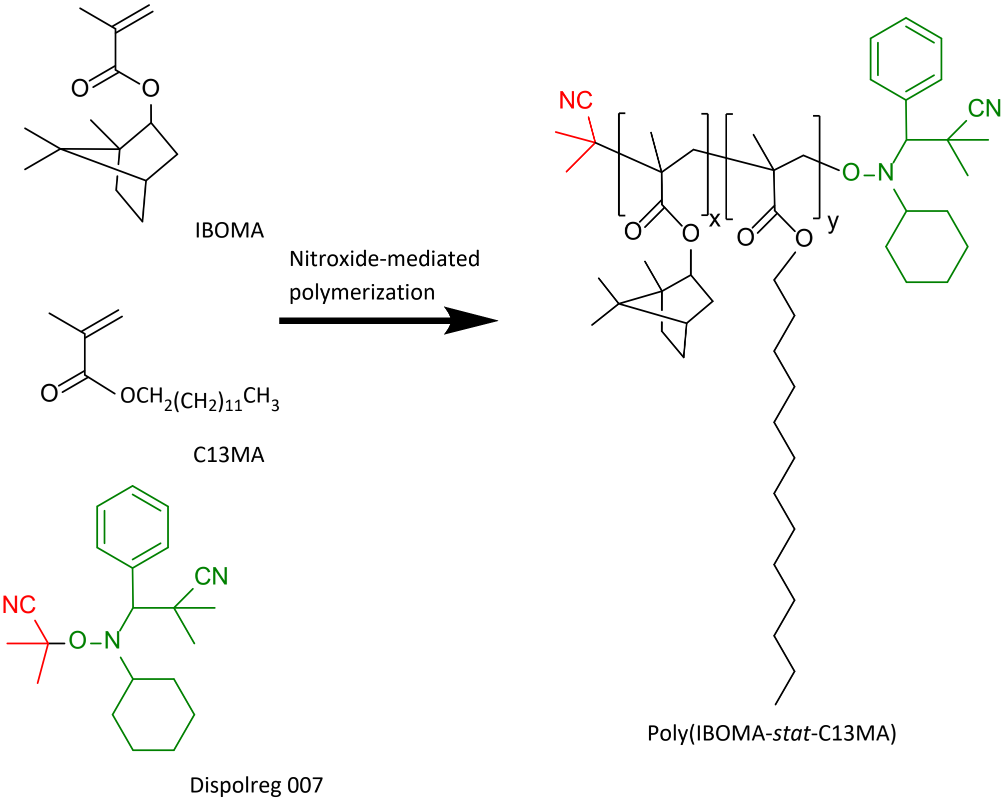

Figure 2. NMP scheme describing the statistical copolymer of IBOMA and C13MA monomers by NMP with the Dispolreg 007 alkoxyamine initiator.

EXPERIMENTAL SECTION

Materials

Isobornyl methacrylate (IBOMA, >99%, Visiomer® Terra IBOMA) and C13 methacrylate (a mixture of methacrylic esters with an average chain length of 13 units, methacrylic ester 13.0, C13MA, >99%, Visiomer® Terra C13-MA) were obtained from Evonik. The monomers were purified to remove the inhibitor by passing them through a column of basic alumina (Brockmann, Type 1, 150 mesh, Sigma Aldrich) and calcium hydride (5 wt% relative to basic alumina, 90-95% reagent, Sigma Aldrich). DOWFAX™ 8390 (alkyldiphenyloxide disulfonate, 35 wt% active content, from Dow Chemical) and n-hexadecane (99%, Sigma Aldrich) were used as received. 3-

(((2-Cyanopropan-2-yl) oxy) - (cyclohexyl) amino)-2, 2-dimethyl-3-phenylpropanenitrile (Dispolreg 007) was synthesized using Ballard *et al.*'s procedure[48]. Methanol (MeOH, >99%), tetrahydrofuran (THF, 99.9%, HPLC grade) and toluene (>99%) were purchased from Fisher Scientific and used as received. The deuterated chloroform ($CDCl_3$, ≥99%) was received from Cambridge Isotopes Laboratory for ^1H NMR tests. All the reactions were conducted under nitrogen atmosphere with high purity (99.99%, Praxair).

Methods

Molecular weight distribution of samples were determined by gel permeation chromatography (GPC, Waters Breeze) relative to PMMA standards without any filtration or purification at 40 °C. Three Waters HR Styragel® GPC columns (HR 1 with molecular weight measurement range of $10^2 – 5 \times 10^3$ g mol^{-1}, HR 2 with molecular weight measurement range of $5 \times 10^2 – 2 \times 10^4$ g mol^{-1} and HR 4 with molecular weight measurement range of $5 \times 10^3 – 6 \times 10^5$ g mol^{-1}, for THF solvent) and a guard column were used. Samples were diluted in THF (HPLC grade) to a concentration of approximately 5 mg ml^{-1}. To measure the Z-average particle size of samples, dynamic light scattering (DLS), was performed using a Malvern Zetasizer Nano- ZS. This instrument was equipped with a 4 mW He–Ne laser at 633 nm and an avalanche photodiode detector. The measurement angle was 173° and temperature was at 25 °C. The samples were diluted to the concentration of 0.01-1000 mg ml^{-1} (10^{-3} – 1 % mass) to prepare them for particle size measurement.

Conversions were determined by ^1H NMR (Varian NMR Mercury spectrometer, 300 MHz, 32 scans, using $CDCl_3$ deuterated solvent) for samples from solution polymerization and gravimetrically for emulsion samples. The final composition for all the polymer samples were also measured by ^{1}H NMR using the same conditions.

To measure the conversions gravimetrically, the samples were dried under ambient conditions in a fume hood for one day and then dried completely for 12 hours under vacuum at room temperature. The dried samples were dissolved in a small amount of toluene and methanol was added to the vials to precipitate the polymer. The supernatant was decanted from the vials to separate the unreacted monomers from the polymers in each sample. Finally, the samples were dried again at atmospheric pressure and room temperature for 12 hours and then dried completely for another 12 hours under vacuum. The same procedure was done for all the copolymers produced in emulsion to prepare them for further mechanical and thermal studies. The conversion was calculated from the Equation (1) for all the emulsion samples:

$$X = \frac{\mathrm{m_{precipitated}}}{\mathrm{m_{sample}}} \cdot \frac{\mathrm{m_{solution}}}{\mathrm{m_{solute}}} \cdot 100 \tag{1}$$

where X is the monomer conversion (%); $m_{precipitated}$ is the mass of the sample after the drying and precipitation process; m_{sample} is the mass of sample before drying (the samples were directly taken from the latex); m_{solute} equals the sum of the masses of the monomers, surfactant, costabilizer and initiator in the latex; and $m_{solution}$ is the overall mass of the prepared latex. (In this study, $\frac{\mathrm{m_{solution}}}{\mathrm{m_{solute}}} = 4$). To determine the conversion via ^{1}H NMR results, Equation (2) was used:

$$X = X_{\mathrm{IBOMA}} f_{\mathrm{IBOMA,0}} + X_{\mathrm{C13MA}} f_{\mathrm{C13MA,0}} \tag{2}$$

where X_{IBOMA} and X_{C13MA} are the individual conversions of IBOMA and C13MA monomers, respectively while $f_{\mathrm{IBOMA,0}}$ and $f_{\mathrm{C13MA,0}}$ are the initial molar fractions of IBOMA and C13MA monomers in the system (a sample ^{1}H NMR spectra for copolymerization of IBOMA and C13MA in toluene is available in Supplementary Information).

Thermogravimetric analysis (TGA) was carried out for all of the samples (previously dried as indicated above) using a TA Instruments TGA Q500TM under nitrogen flow at a ramp rate of 15 °C min^{-1} from 25 to 500 °C in aluminium pans to find the decomposition temperature (T_d). Differential scanning calorimetry (DSC, Q2000TM from TA Instruments) was performed under nitrogen to obtain the glass transition temperature (T_g) of samples. The three scans per cycle (heat/cool/heat) method was used at a heating rate of 15 °C min^{-1} and cooling rate of 50 °C min^{-1} in the temperature range of -90 to 170 °C to calculate T_gs using the inflection method.

Powder X-ray diffraction (PXRD) was carried out to assess crystallinity of the samples. A Bruker D2 Phaser diffractometer equipped with a LynxEyr linear position sensitive detector (Bruker AXS, Madison, WI, USA) and Ni-filtered CuKα radiation tube was used for this study. The voltage was 40 kV and the current was 40 mA. The results were collected with a step of 0.02° and 0.5 seconds/step in the range of 2θ = 4-50°. The fraction of crystalline to amorphous content was calculated based on the peak area ratios.

Tensile tests were performed with an EZ-test-500N Shimadzu tensile tester. All dumbbell-shaped samples had the necks with approximately 3 mm width and 2 mm thickness and were tested based on ASTM D638 type V[103]. The samples were extended at a rate of 10 mm min^{-1} at room temperature and the reported data are the average of 5 measurements.

Rheological properties of selected samples were done using isothermal frequency sweeps on an Anton Paar MCR 302 rheometer from 1 to 1000 Hz with an amplitude of 1% under N_2 atmosphere at different temperatures (100, 140 and 150 °C). The measurements were performed in dynamic shearing mode using parallel plates (diameter = 25 mm) inside a CTD 450 convection oven. To prepare samples for different measurements, all the polymers were dried completely under vacuum overnight and precipitated in methanol to remove the unreacted monomers. After the precipitation, samples were dried again under vacuum for 24 hours at room temperature.

NMP of Isobornyl Methacrylate and C13 Methacrylate in Toluene Using Dispolreg 007 Initiator

To study the kinetics of polymerization and properties of copolymers with different ratios of IBOMA and C13MA, all the solution polymerizations were performed in a 15 ml, three-neck round-bottom glass flask connected to a reflux condenser which had fluid circulating at 3°C (the condenser was filled with a mixture of ethylene glycol/distilled water (20/80 vol%)). Target average molecular weight for all the studies in toluene solvent was 25 kg mol^{-1}. The bio-based monomers (IBOMA, C13MA or a mixture of them) and Dispolreg 007 alkoxyamine were dissolved in 50 wt% toluene solvent. The final solution was stirred for 10 minutes and was transferred into the reactor. A thermocouple was placed inside the reactor and connected to a temperature controller to control the reaction temperature during the polymerization. To provide a constant mixing in the reactor, a magnetic stir bar was added to the reactor and the reactor was placed inside a heating mantle on a magnetic stirrer. The reactants were deoxygenated by a purge of ultrapure nitrogen prior to polymerization for 30 minutes at room temperature. The nitrogen purging continued during the polymerization. At this point, the system was heated at a rate of about 10 °C.min^{-1} and the time when the reactor temperature reached 75 °C was taken as the commencement of the reaction. Samples were taken periodically during the reactions until a prescribed time or when the solution was too viscous to take samples using the sampling syringe.

To stop the reactions, the reactor was removed from heating mantle and cooled down to room temperature.

Chain-Extension of Poly(IBOMA) Macroinitiator with C13MA

To check the chain end fidelity of polymer chains, chain-extension of poly(IBOMA) macroinitiators were conducted using a second batch of C13MA monomer. First, the homopolymerization of IBOMA was conducted at 100 °C with the same experimental procedure presented earlier. However, the reaction was stopped at 90 minutes to ensure polymer chains had highly active ends (X=25%, M_n = 13.6 kg mol^{-1}, $Đ$ = 1.47). The macroinitiator was then precipitated in methanol to remove the unreacted monomers. Next, 0.9259 g of poly(IBOMA) macroinitiator (0.068 mmol), C13MA (2.7777 g, 10.364 mmol) and toluene (50 wt%, 3.7036 g, 40.195 mmol) were mixed for 10 min and added to the reactor. The reactor was sealed, and the solution was purged with ultra-pure nitrogen for 30 min before the reaction was started by heating up to the desired temperature. The nitrogen purging continued during the synthesis to avoid the termination reactions. A temperature of 100 °C and $M_{n,target}$ = 40 kg mol^{-1} were used for the chain-extension reaction. The polymerization continued for 3 hours to synthesize block copolymer of IBOMA and C13MA. Finally, the reaction was stopped, and the polymer was precipitated in methanol (X=55%, M_n = 37.1 kg mol^{-1}, $Đ$ = 1.93, F_{IBOMA} = 0.22).

Miniemulsion Polymerization of IBOMA and C13MA Using Dispolreg 007 Initiator

Miniemulsions were prepared based on the formulation in Table 1. The $M_{n,target}$ for all the studies in emulsion was set to 45 kg mol^{-1}. DOWFAX™ 8390 is a biodegradable ionic surfactant with low volatility and low sorption to soils, which makes it a good candidate for a green miniemulsion polymerization [104-106]. N-hexadecane was added as the costabilizer to the miniemulsion system to inhibit Ostwald ripening and improve the colloidal stability of latex [107]. N-Hexadecane is also biodegradable and it can be extracted from sustainable bio-sources such as long pepper[108, 109]. In order to prepare the system for polymerization, monomers, n-hexadecane and Dispolreg 007 were mixed together for 10 minutes. The aqueous solution was prepared separately by dissolving DOWFAX™ 8390 as the surfactant in distilled water and stirring it for 10 minutes. Then, two solutions were mixed together for 15 minutes and the resulting emulsion was sonicated using a Hielscher sonicator (model UP200S, 50% duty cycle and amplitude 70%) for 10 minutes in a cold water bath. The final emulsion was added to a 50 ml three-neck round-bottom glass flask connected to a reflux condenser that was cooled to 3 °C. The condenser was cooled with a mixture of ethylene glycol/distilled water (20/80 vol%) from a Polyscience recirculating chiller Model MX7LR-20-A11B. A thermocouple was placed inside the reactor and connected to a temperature controller to control the reaction temperature during the polymerization. To provide mixing of the contents inside the reactor, a magnetic stir bar was added to the reactor and the reactor was placed inside a heating mantle on a magnetic stirrer. The reactants were deoxygenated by a purge of ultrapure nitrogen prior to polymerization for 30 minutes at room temperature. The nitrogen purging continued during the polymerization. At this point, the system was heated at a rate of about 10 $°\mathrm{C.min}^{-1}$ and the time when the reactor temperature reached 75 °C was taken as the commencement of the reaction. Samples were taken periodically during the reaction for measurement of molecular weight, conversion and particle size.

Table 1. Typical recipe for the nitroxide-mediated miniemulsion polymerization of Isobornyl Methacrylate (IBOMA) and C13 Methacrylate (C13MA).

Component	**Amount**
Monomer (1) – IBOMA	Varies based on the experiment (0-1.082 M)
Monomer (2) – C13MA	Varies based on the experiment (0-0.872 M)

Alkoxyamine (Dispolreg 007)	0.005 M
DOWFAX™ 8390	2 wbm%
n-Hexadecane	0.8 wbm%
Water	75 wt%

Chain Extension of Poly(C13MA) with IBOMA Monomer in Emulsion Using Dispolreg 007 Initiator

The seed latex of poly(C13MA) was prepared in a 100 ml three-neck round-bottom glass flask connected to a reflux condenser and under nitrogen atmosphere for 150 minutes at 90° C. The recipe for preparation of poly(C13MA) seed latex is described in Table 2. The magnetic stirrer was added, and the temperature was controlled using a thermocouple. In the next step, IBOMA monomer (IBOMA:C13MA = 1:1 weight ratio) was bubbled with nitrogen for 30 minutes and added to the flask in a single shot. The polymerization continued for another 120 minutes under the same conditions to prepare the gradient copolymer of C13MA and IBOMA in miniemulsion system.

Table 2. Recipe for preparation of seed latex of poly(C13MA) at 90° C (10 wt% solid content, Dispolreg 007 initiator)

Component	**Amount**
C13 methacrylate (C13MA)	0.381 M
Alkoxyamine (Dispolreg 007)	0.004 M
DOWFAX™ 8390	5 wbm%
n-Hexadecane	1 wbm%
Water	89 wt%

RESULTS AND DISCUSSION

NMP of IBOMA and C13MA in Toluene

The NMP of IBOMA and C13MA monomers was conducted first in toluene to study the polymerization kinetics in organic solvent as a base for comparison with an emulsion-based system. The nitroxide mediated copolymerization of IBOMA and C13MA was carried out in toluene using Dispolreg 007 initiator without using any controlling comonomers. Table 3 represents all the studies in toluene using Dispolreg 007 initiator. First, the effect of temperature on the homopolymerization of IBOMA and C13MA was studied (please refer to Supplementary Information Section 2). Then, the effect of different ratios of IBOMA:C13MA on the kinetics of polymerization was investigated.

Table 3. Summary of experiments for nitroxide-mediated copolymerization of IBOMA/C13MA mixtures in toluene solvent using Dispolreg 007 initiator.

Experiment ID	Reaction time (min)	$M_{n,\text{final}}$ [c] (kg mol^{-1})	X [d] (%)	[Dispolreg 007] (M)	$[\text{IBOMA}]_0$ (M)	$[\text{C13MA}]_0$ (M)	Đ [c]	T [e] (°C)
IBOMA100-S-90C[a]	90	13.6	25.0	0.018	2.054	0	1.47	90
IBOMA100-S-100C	90	16.5	69.1	0.018	2.054	0	1.54	100
IBOMA100-S-110C	60	13.9	83.6	0.018	2.054	0	1.66	110
C13MA100-S-90C	210	16.9	43.7	0.017	0	1.609	1.45	90
C13MA100-S-100C	180	24.2	82.8	0.017	0	1.609	1.39	100
C13MA100-S-110C	150	20.0	89.6	0.017	0	1.609	1.59	110
IBOMA80/C13MA20-S[b]	120	23.6	76.3	0.018	1.559	0.390	1.56	100
IBOMA60/C13MA40-S	120	25.0	78.3	0.018	1.110	0.740	1.54	100
IBOMA50/C13MA50-S	120	26.1	69.9	0.018	0.902	0.902	1.61	100
IBOMA40/C13MA60-S	120	24.1	71.2	0.018	0.704	1.057	1.52	100
IBOMA30/C13MA70-S	120	26.5	77.0	0.018	0.516	1.204	1.54	100
IBOMA20/C13MA80-S	120	27.3	70.0	0.017	0.336	1.344	1.50	100
IBOMA10/C13MA90-S	150	19.8	77.3	0.017	0.164	1.479	1.52	100

[a] Solution polymerization of 100 mol% IBOMA in the initial feed composition at 90 °C (solvent: toluene). [b] Solution polymerization of monomers with initial feed composition of 80 mol% IBOMA and 20 mol% C13MA (solvent: toluene). [c] The final number-average molecular weight (M_n) and dispersity (Đ) were reported from GPC relative to PMMA standards in THF at 40 °C. The target number-average molecular weight $M_{n,\text{target}}$ for all the polymerization in toluene was 25 kg mol^{-1}. [d] Overall monomer conversion measured by ^{1}H NMR. [e] The reaction temperature units (°C).

Poly(IBOMA-*stat*-C13MA) Solution Copolymerization by NMP

IBOMA/C13MA mixtures, with initial IBOMA molar feed compositions f_{IBOMA} = 0.1-0.8 were copolymerized by NMP using Dispolreg 007 initiator in 50 wt% toluene at the optimal polymerization temperature of 100 °C (This was studied in the range of 90-110 °C; please see the Supplementary Information Section 2). Table 3 presents the experimental conditions for this series of syntheses. As Figure 3 indicates, the semi-logarithmic kinetic plots with time was linear for all the reactions. The apparent slopes do not show a significant difference between different IBOMA/C13MA copolymerizations. This is in accordance with our previous results for NMP of IBOMA and C13MA using BB and 10 mol% AN controlling comonomer [83]. In addition, the values of the apparent rate constant $k_P[P^\bullet]$ (k_P = propagation rate constant, $[P^\bullet]$ is the concentration of polymer with radical chain ends) for the experiments at 100 °C using Dispolreg 007 initiator are lower than the values for BB (with 10 mol% AN as the controlling comonomer) in our previous study, indicating a slower polymerization rate when using Dispolreg 007 compared to BB[50]. It should be noted using a small amount of AN comonomer is essential to use BB initiator, however when using Dispolreg 007, no controlling comonomer is required and thus it is difficult to make a direct comparison between the two systems[83]. The $Đ$ of samples shown in Figure 3(b) was in the range of $1.19 < Đ < 1.61$ which generally decreased as the molar ratio of C13MA monomer increased in the system. M_n plots versus conversion were linear at low conversion ($X \sim < 40\%$) and all of them have an over-prediction in terms of adherence to the theoretical line due to slow initiation of the Dispolreg 007 initiator[110]. At higher conversions ($X > 40\%$), the slope of M_n versus conversion plots slightly decreases. This could be ascribed to the onset of irreversible termination reactions which decreases the concentration of macro-radicals $[\mathrm{P}^\bullet]$ and possible complete consumption of the initial alkoxyamines at higher conversions.

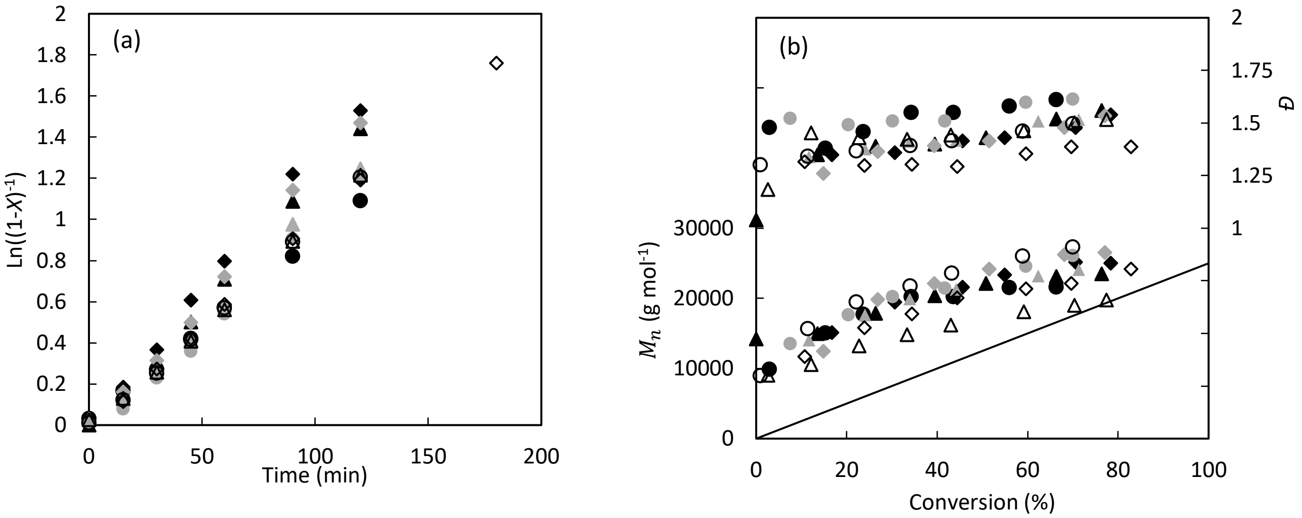

Figure 3. NMP to produce poly(IBOMA-*stat*-C13MA) copolymers using Dispolreg 007 initiator in toluene (50 wt%) at 100 °C and $M_{n,target}$ = 25 kg mol^{-1}. (a) Semi-logarithmic kinetic plots of ln[(1-X)$^{-1}$] (X= monomer conversion) versus reaction time (b) The evolution of M_n and $Đ$ with conversion (X). IBOMA100-S-100C (filled circles, ●); IBOMA80/C13MA20-S (filled triangles, ▲); IBOMA60/C13MA40-S (filled diamonds, ♦); IBOMA50/C13MA50-S (gray circles, ●); IBOMA40/C13MA60-S (gray triangles, ▲); IBOMA30/C13MA70-S (gray diamonds, ♦); IBOMA20/C13MA80-S (open circles, ○); IBOMA10/C13MA90-S (open triangles, Δ); C13MA100-S-100C (open diamonds, ◊).

Effect of Feed Composition on Poly(IBOMA-*stat*-C13MA) Solution Copolymerization by Dispolreg 007

In addition to kinetic studies, the influence of feed composition on the copolymer composition was studied in homogenous toluene solution at 100 °C. This was done to predict thermal and mechanical properties of copolymers that are subsequently made in emulsion. The composition of the copolymers was determined by ^{1}H NMR at the early stages of the copolymerization to extract the low-conversion data (X<10% for every copolymerization, Table S1, Supplementary Information).

A non-linear regression fit to the Mayo-Lewis equation was used to extract the reactivity ratios of poly(IBOMA-*stat*-C13MA) and the uncertainties were provided from the standard errors of the parameters in the calculation[111]. Employing the terminal copolymerization model, it is always presumed that the reactivity of an active center depends on the nature of the terminal monomer unit of the propagating chain[112]. The commercial software MATLAB R2016a was used to solve the Mayo-Lewis equation[113]:

$$F_{IBOMA} = \frac{r_{IBOMA} f_{IBOMA,0}^{2} + f_{IBOMA,0} f_{C13MA,0}}{r_{IBOMA} f_{IBOMA,0}^{2} + 2 f_{C13MA,0} f_{IBOMA,0} + r_{IBOMA,0} f_{TDMA,0}^{2}} \tag{3}$$

The statistical fit yielded reactivity ratios $r_{IBOMA} = 0.89 \pm 0.13$ and $r_{C13MA} = 1.80 \pm 0.21$, suggesting the C13MA monomer is slightly more reactive than IBOMA towards both propagating species (–IBOMA$^{\bullet}$ and –C13MA$^{\bullet}$). The Mayo-Lewis plot (Figure 4) indicates that poly(IBOMA-*stat*-C13MA) formed instantaneously by solution copolymerization was always slightly richer in C13MA without any azeotropic composition. Although IBOMA and C13MA reactivity ratios have not been reported, they can be compared to similar methacrylate copolymerizations. Lauryl methacrylate (LMA) is similar to C13MA and there are a few cases of LMA copolymerizations with other methacrylates. For instance, the reactivity ratios of lauryl methacrylate (LMA) and methyl methacrylate (MMA) in 1,1,2-trichloro-1,2,2, trifluoroethane at 60 °C were reported as $r_{LMA} = 0.84 \pm 0.10$ and $r_{MMA} = 1.22 \pm 0.14$[114], while using conventional free radical polymerization in toluene at 70 °C for the same monomers resulted in $r_{MMA} = 1.12 \pm 0.01$ and $r_{LMA} = 1.19 \pm 0.01$[115]. In another study, the reactivity ratios of IBOMA and tetrahydrofurfuryl methacrylate (THFMA) from photo copolymerization experiments were $r_{IBOMA} = 0.47 \pm 0.10$ and $r_{THFMA} = 2.51 \pm 0.35$[116]. For the ATRP of IBOMA with 4-methoxybenzyl methacrylate (MBMA) at 100 °C in bulk, the reactivity ratios were $r_{IBOMA} = 0.89 \pm 0.01$ and $r_{MBMA} = 0.64 \pm 0.01$ [117].

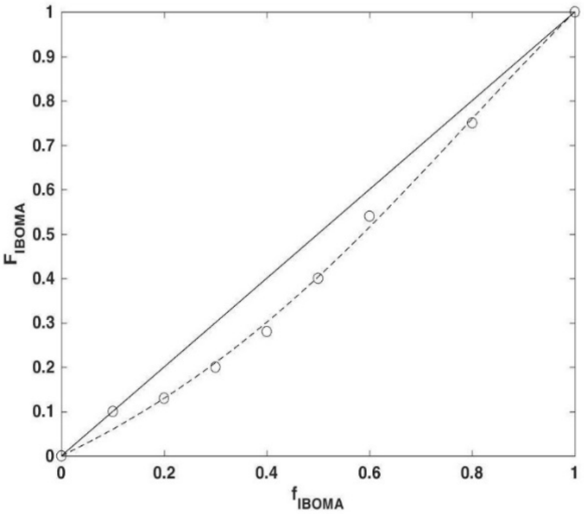

Figure 4. Mayo-Lewis plot of copolymer composition with respect to IBOMA molar fraction at low conversion or instantaneous composition ($F_{IBOMA,i}$) versus initial IBOMA feed composition ($f_{IBOMA} \approx f_{\mathrm{IBOMA},0}$). The open circles represent the experimental data and the dashed line shows the trend line. The straight line is associated with the azeotropic composition ($F_{IBOMA} = f_{IBOMA}$). The copolymerization was performed at 100 °C using Dispolreg 007 initiator in 50 wt% toluene. $F_{IBOMA,i}$ of copolymers is available in Table S1 in Supplementary Information.

Chain-Extension of Poly(IBOMA) Macroinitiator with C13MA

The chain-end fidelity of polymer chains and the possibility of making block copolymers was tested by the chain-extension of poly(IBOMA) macroinitiators using a fresh batch of C13MA. The formulation and kinetic data of chain-extensions are available in Table 4. The poly(IBOMA) macroinitiator was prepared at 100 °C (X = 25%, M_n = 13.5 kg mol^{-1} and $Đ$ = 1.47). Then, the macroinitiator was mixed with C13MA and the chain-extension reaction continued for 180 minutes at the same temperature. The GPC chromatograms of the chain-extension are presented in Figure 5. Accordingly, a clear, monomodal shift of M_n toward higher molecular weight was observed, indicating nearly simultaneous growth of all chains. The increased $Đ$ is due to the appearance of the lower molecular weight tail, which suggests some dead macroinitiator was present. For the final sample chromatogram (at 180 minutes after the chain extension), multiple Gaussian peak fitting was carried out to estimate the percentage of dead polymer chains in the final sample. According to the fitting analysis presented in Figure S2 (Supplementary Information) after three hours of chain-extension, 27.5 % of the initiating polymer chains were estimated to be dead. This shows that the majority of polymer chains were active up to 55% conversion in organic solvent. This provided a basis of what to expect in emulsion conditions and we hypothesized compartmentalization effects inherent in the miniemulsion process to provide improved chain activity to higher conversions[64, 72, 73].

Table 4. Chain-extension of IBOMA macroinitiator with C13MA in 50 w% toluene at 100 °C for 3 hours and molecular characterization of the resulting chain-extended product.

A. Macroinitiator

Experiment ID	X[a] (%)	[Dispolreg] (M)	[IBOMA] (M)	[Toluene] (M)	M_n[b] (kg mol^{-1})	$M_{n,theo}$[c] (kg mol^{-1})	$Đ$[b]	Time[d] (min)
Poly(IBOMA)-macroinitiator	25	0.020	2.212	5.409	13.6	25	1.47	90

B. Formulation and Characterization of Chain-Extension

Experiment ID	[Macroinitiator] (M)	X[a] (%)	F_{IBOMA}[e]	[Toluene] (M)	M_n[b] (kg mol^{-1})	[C13MA] (mmol)	$M_{n,theo}$[f] (kg mol^{-1})	$Đ$[b]	Time[d] (min)
Poly(IBOMA-*b*-C13MA)	0.009	55	0.22	5.385	37.1	1.389	40	1.93	180

[a] Overall monomer conversion measured by ^{1}H NMR. [b] The final number average molecular weight (M_n) and dispersity ($Đ$) were measured by GPC relative to PMMA standards at 40 °C in THF. [c] The target number average molecular weight to synthesize poly(IBOMA)-macroinitiator. [d] The reaction time (minutes). [e] Molar fraction of IBOMA in the polymer chain. [f] The target number average molecular weight for the whole block copolymer

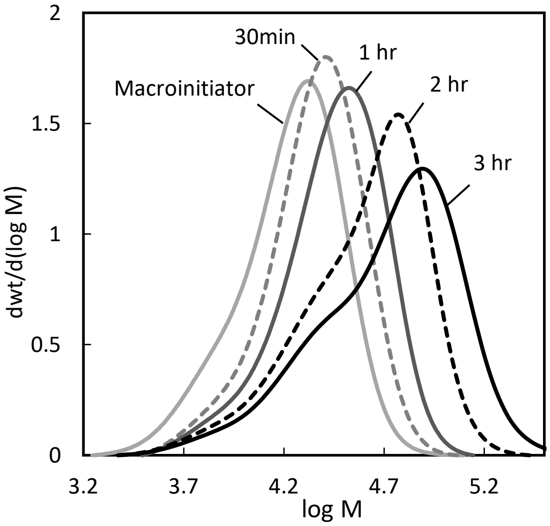

Figure 5. GPC traces for chain-extension of poly(IBOMA) macroinitiator ($M_n = 13.6$ kg mol^{-1} and $Đ = 1.47$) with C13MA. Chain-extension was done in 50 wt% toluene at 100 °C. The gray solid line is the macro initiator while the black solid line is the chain-extended product with $M_n = 40.7$ kg mol^{-1} and $Đ = 1.93$ (Dispersity is reported for the overall peak, containing the active and dead polymers). Full characterization data for the samples shown is provided in Table 4.

Copolymerization of IBOMA/C13MA by Nitroxide-Mediated Miniemulsion Polymerization Using Dispolreg 007 Initiator

The oil-soluble Dispolreg 007 initiator required balancing the amount of surfactant and costabilizer relative to other NMP miniemulsion studies [56, 118]. Accordingly, the amount of DOWFAX™ 8390 surfactant that should be added is at least 2 to 5 wbm% (weight based on the monomers) to prevent coagulation[119]. Since reduction of the amount of surfactant in the latex is desired due to environmental concerns (eg. biodegradability, toxic effects on aquatic organisms), addition of only 2 wbm% of DOWFAX™ 8390 was applied for this study [120-123]. The miniemulsion polymerization was conducted by adding 2 wt% Dowfax™ 8390 relative to monomer as the surfactant and 0.8

wt% hexadecane relative to monomer as the costabilizer. The highly hydrophobic monomers of IBOMA and specifically C13MA acted as polymerizable costabilizers inside particles, which helped retarding Ostwald ripening and compensates the need for higher concentration of n-hexadecane. The monomer content in all latexes was 24.14 wt% and $M_{n,target}$ of 45 kg mol^{-1} was considered for all the polymerizations. Figure 6 graphically displays the system used for this study. Table 5 lists all the studies for the miniemulsion polymerization of monomer feeds with different ratios of IBOMA/C13MA using Dispolreg 007 initiator.

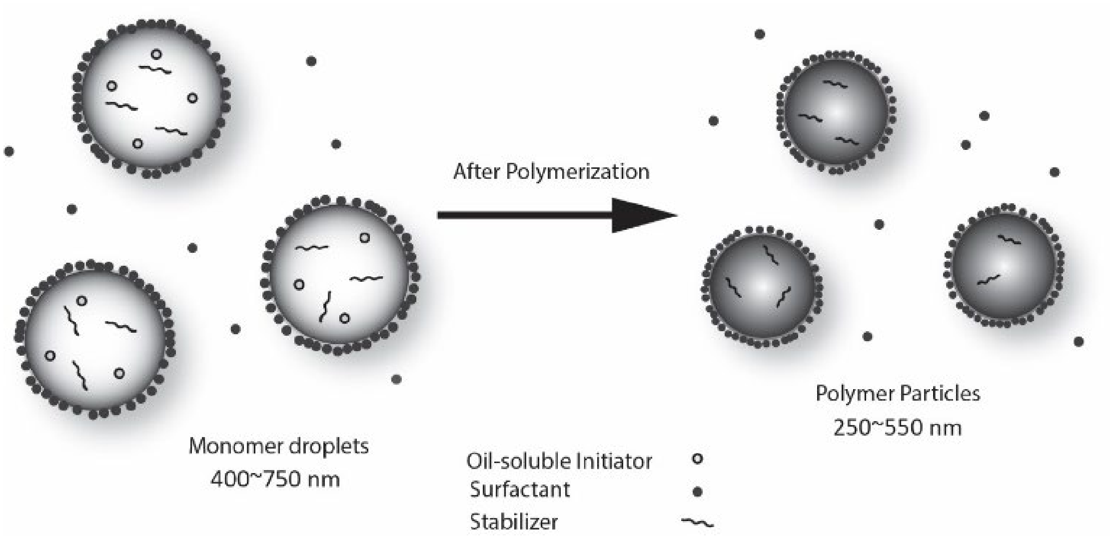

Figure 6. The schematic of nitroxide-mediated miniemulsion polymerization using oil-soluble Dispolreg 007 initiator.

Table 5. Summary of experiments for nitroxide-mediated miniemulsion polymerization of IBOMA/C13MA copolymerization.

Experiment ID	$M_{n,final}$ [b] (kg mol^{-1})	X [c] (%)	[Dispolreg 007]$_0$ (M)	[IBOMA]$_0$ (M)	[C13MA]$_0$ (M)	Đ [b]	T [d] (°C)	D$_z$ [e] (nm)
IBOMA100 [a]	42.2	82.7	0.005	1.082	0	1.50	90	548
IBOMA100-83C	39.3	67.6	0.005	1.082	0	1.58	83	441
IBOMA100-100C	33.5	64.2	0.005	1.082	0	1.54	100	526
IBOMA90/C13MA10	53.9	91.1	0.005	0.951	0.106	1.70	90	415
IBOMA80/C13MA20	57.8	83.4	0.005	0.826	0.206	1.68	90	353
IBOMA70/C13MA30	46.8	85.3	0.005	0.706	0.303	1.62	90	331
IBOMA60/C13MA40	56.2	92.4	0.005	0.592	0.395	1.63	90	291

IBOMA50/C13MA50	50.8	87.8	0.005	0.483	0.483	1.72	90	327
IBOMA40/C13MA60	64.2	88.8	0.005	0.378	0.567	1.65	90	481
IBOMA30/C13MA70	67.9	94.0	0.005	0.278	0.648	1.66	90	276
IBOMA20/C13MA80	63.8	92.7	0.005	0.181	0.726	1.68	90	270
IBOMA10/C13MA90	61.1	92.6	0.005	0.089	0.800	1.73	90	306
C13MA100	48.9	73.3	0.005	0	0.872	1.55	90	472

[a] The miniemulsion polymerization of IBOMA and C13MA monomers with the initial feed composition of 100 mol% IBOMA and 0 mol% C13MA. The monomer content for all the emulsions was 24.14 wt%. [b] The final number average molecular weight (M_n) and dispersity ($Đ$) were measured by GPC with PMMA standards in THF at 40 °C. The target number average molecular weight ($M_{n,target}$) for all the miniemulsion polymerizations was 45 kg mol^{-1}. [c] Overall monomer conversion measured gravimetrically. [d] The reaction temperature (°C). [e] Final Z-average particle size (nm).

Firstly, the miniemulsion homopolymerization of IBOMA was conducted at different temperatures using the Dispolreg 007 to confirm the optimum reaction temperature. Figure S3 in the Supplementary Information displays the kinetic results at three different temperatures of 83, 90 and 100 °C for homopolymerization of IBOMA in toluene. The lowest temperature (83° C) was used to compare the results for the polymerization of methacrylates conducted by Ballard and co-workers using the Dispolreg 007 alkoxyamine[47]. Figure S3(a) illustrates the linear trends for the polymerizations at 90 and 100 °C. However, the semi-logarithmic kinetic plots of $\ln[(1-X)^{-1}]$ (X= monomer conversion) versus reaction time was not linear at 83° C due to the slow initiation of Dispolreg 007 initiator. The polymerization rate of IBOMA at 83 °C was much lower than at 90 or 100 °C, as the Dispolreg 007 initiator decomposes much more readily at elevated temperatures [48, 124]. At 100 °C, the reaction was very fast and stopped at 45 minutes as particle coagulation and precipitation was observed, indicating the emulsion lost its stability (overall conversion = 64%, $Đ$ = 1.54 and $M_{n,final}$ = 33 kg mol^{-1}). This can be due to some evaporation of water at this temperature that alters the concentration of monomer/polymer in the surrounding aqueous medium and destabilizes the system. The evolution of molecular weight with overall conversion was not linear in all cases and it is higher than that predicted, especially at lower conversions. This is in agreement with previous studies of NMP using Dispolreg 007 initiator which showed slow initiation due to a strong penultimate effect [48, 58]. The molecular weight distributions were somewhat broad ($Đ$ <

1.64) but comparable with the results for homogeneous polymerization in toluene. The final average particle size ranged from 441 to 548 nm. Based on these results, the optimal temperature was chosen as 90 °C, which balanced high overall conversion (X = 82%) with a relatively low dispersity ($Đ$ < 1.57), while still remaining colloidally stable. Therefore, ensuing binary copolymerizations in emulsion were done using these conditions.

The Copolymerization of Different Ratios of IBOMA/C13MA Using Dispolreg 007 Initiator in Emulsion

After finding an acceptable temperature from the homopolymerization kinetic studies, the copolymerization of different ratios of IBOMA and C13MA was conducted in emulsion by NMP. Figure 7(a) represents the semi-logarithmic kinetic plots of $\ln[(1-X)^{-1}]$ versus time for different initial ratios of IBOMA and C13MA monomers. As shown in Figure 7(a), the kinetic plots were linear in all cases and no significant increase in polymerization rate was observed for different ratios of $[\text{IBOMA}]_0/[\text{C13MA}]_0$ in the system for the copolymerization.

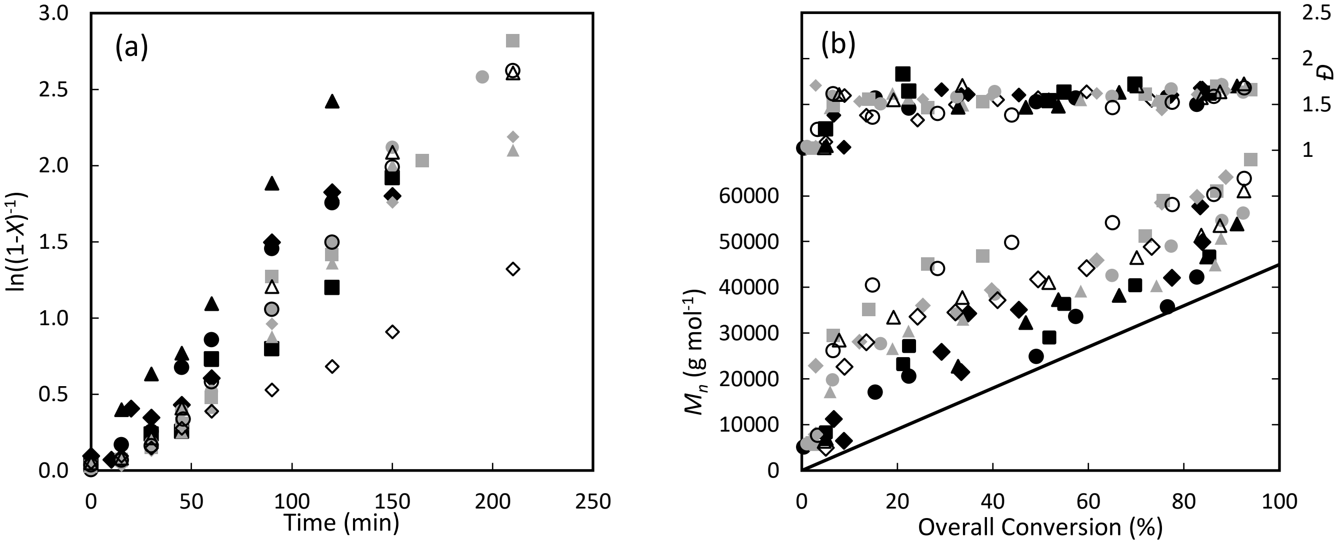

Figure 7. The miniemulsion polymerization of different ratios of IBOMA/C13MA using Dispolreg 007 initiator (a) Semi-logarithmic kinetic plots of $\ln[(1-X)^{-1}]$ (X= monomer conversion) versus reaction time (b) Number average molecular weight M_n and dispersity $Đ$ versus conversion (X). IBOMA100 (filled circles, ●); IBOMA90/C13MA10 (filled triangles, ▲); IBOMA80/C13MA20 (filled diamonds, ♦); IBOMA70/C13MA30 (filled squares, ■); IBOMA60/C13MA40 (gray circles, ●); IBOMA50/C13MA50 (gray triangles, ▲); IBOMA40/C13MA60 (gray diamonds, ♦); IBOMA30/C13MA70 (gray squares, ■); IBOMA20/C13MA80 (open circles, ○); IBOMA10/C13MA90 (open triangles, Δ); C13MA100 (open diamonds, ◊).

Based on the results shown in Figure 7(b), it can be assumed that increasing the ratio of $[\mathrm{IBOMA}]_0/[\mathrm{C13MA}]_0$ slightly increases control over the polymerization. This can be due to the comparatively lower propagation rate constant k_p for IBOMA, which decreases the propagation rate for reactions with higher [IBOMA] and improves the control over the polymerization[83]. As it was shown in Figure 7(b), the reactions with higher initial concentrations of C13MA deviate more from the theoretical line in the M_n versus conversion (X) plot and it seems that decreasing the initial amount of IBOMA causes the control loss. It should be noted that the deviation is partly due to the calibration against PMMA standards without applying the Mark-Houwink-Sakurada coefficients for C13MA and IBOMA homopolymers as they were not available for C13MA homopolymers. This, along with the slow initiation of Dispolreg 007 alkoxyamine at lower conversions (overall conversion < 25%) results in higher M_n at higher conversions, especially for the copolymers with higher [C13MA]. Interestingly, this phenomenon is only pronounced in the miniemulsion system, where the polymerization occurs inside the particles. This can be due to higher reaction temperature for polymerization in toluene (the reaction temperature in toluene and emulsion are

100 and 90 °C, respectively), the variation of particle sizes for different reactions in emulsion and also higher $M_{n,target}$ for emulsions compared to the toluene-based system ($M_{n,target,emulsion}$ = 45 kg mol^{-1} versus $M_{n,target,toluene}$ = 25 kg mol^{-1}). Final $Đ$ for miniemulsion homopolymerization of IBOMA and C13MA was $Đ_{poly(IBOMA)} = 1.50$ and $Đ_{poly(C13MA)} = 1.55$, respectively. For all the copolymers of IBOMA and C13MA studied in the emulsion system, the final $Đ$ was in the range of $1.62 < Đ < 1.72$ (Figure 7(b)). This showed that the final dispersity of emulsion samples was slightly higher than the final $Đ$ of samples prepared in toluene ($1.50 < Đ < 1.61$), considering that the $M_{n,target}$ was different in these systems. Elsewhere, compartmentalization of nitroxides and radicals has an influence on polymerization and termination rates within the monomer particles and resulted in higher dispersity of polymers made in an emulsion system [28, 64].

Study of the Particle Size in Miniemulsion NMP of IBOMA/C13MA

The Z-average particle size of latex samples was determined by DLS. All the samples were diluted in deionized water just before the test without filtration. Initially, the effect of addition of costabilizer (n-hexadecane) and surfactant on particle size was studied. As the oil-soluble Dispolreg 007 alkoxyamine was used in the system, the initiation reaction occurred inside monomer droplets and the surfactant stabilized the system[54, 58]. First, the effect of temperature on the particle size was studied by NMP of IBOMA in emulsion and the results are presented in Figure S4 (a). As shown in Figure S4 (a) and (b), the coagulation in the final emulsions was not significant and the final particle size in all experiments was smaller than the initial particle size [58]. Sometimes, the Z-averaged particle size fluctuated as the polymerization continued, suggesting the presence of a low concentration of micron-sized particles due to the coagulation of monomer droplets or polymer particles[58]. Figure S4 (b) illustrates the evolution of particle size during the course of each polymerization for different initial molar ratios of IBOMA:C13MA. The particle size during the copolymerization generally decreased with increasing C13MA concentration, with most particles ~ 400-500 nm for richer IBOMA compositions and decreasing to ~ 300-400 nm for lower IBOMA compositions. Interestingly, the C13MA homopolymerization in emulsion had slightly larger particle sizes compared to those with some IBOMA. The general decreases in particle size as C13MA composition increased shows the effect of the long-chain n-alkyl group in the C13MA monomers which can act as a costabilizer in the monomer particles, preventing diffusional degradation and improving the colloidal stability [125-127]. It is worth mentioning that the polymer latexes were colloidally stable at room temperature for at least three months (the duration of investigation) and no polymer precipitation nor change in particle size was observed.

Chain Extension of Poly(C13MA) with IBOMA Monomers in Emulsion Using Dispolreg 007 Initiator

Chain extension of poly(C13MA) with IBOMA monomers was conducted to check the chain-end fidelity as well as the possibility of making gradient copolymers in NMP miniemulsion [118]. First, a seed latex of poly(C13MA) with 10 wt% solid content was prepared at 90° C. After 150 minutes of the polymerization, IBOMA was added to the system to make the gradient polymer. Table 6 shows the kinetic data and properties of the gradient miniemulsion polymerization of C13MA and IBOMA. The shift in GPC traces toward higher molecular weights indicates the clean attainment of poly(C13MA-*grad*-IBOMA) copolymer (Figure 8). This is in contrast to the solution polymerization shown in Figure 5 which indicates some tailing. There are several differences and it is difficult to compare the chaine extensions as the macroinitiators were prepared at different conversions (the miniemulsion macrointiator was made to higher conversion) yet had no obvious tailing. It is possible that there are chain transfer effects in solvent that influence the fidelity of the macroinitiator more than any of the factors influencing the miniemulsion polymerization.

Table 6. Chain-extension of poly(C13MA) with IBOMA in miniemulsion system at 90 °C for 2 hours and molecular characterization of the resulting chain-extended product.

A. Macroinitiator

Experiment ID	X^a (%)	[Dispolreg 007]$_0$ (M)	[C13MA]$_0$ (M)	$M_n{}^b$ (kg mol^{-1})	$M_{n,theo}{}^c$ (kg mol^{-1})	$Đ^b$	t^d (min)	D$_z{}^e$ (nm)
Poly(C13MA) seed latex	61	0.004	0.381	34	25	1.55	150	339

B. Formulation and Characterization of Chain-Extension

Experiment ID	X^a (%)	$F_{IBOMA}{}^f$	$M_n{}^b$ (kg mol^{-1})	[IBOMA]$_0$ (mmol)	$Đ^b$	t^d (min)	D$_z{}^e$ (nm)
Poly(C13MA-*grad*-IBOMA)	87	0.51	54	0.233	1.65	120	345

C. Results for Thermal Characterization by DSC and TGA

	T$_m{}^g$ (°C)	T$_{g,1}{}^g$ (°C)	T$_{g,2}{}^g$ (°C)	T$_{dec,1}{}^h$ (°C)	T$_{dec,max}{}^h$ (°C)	T$_{dec,2}{}^h$ (°C)
Poly(C13MA-*grad*-IBOMA)	-27	-32	76	220	282	470

[a] Overall monomer conversion measured gravimetrically. [b] The final number average molecular weight (M_n) and dispersity ($Đ$) were measured by GPC with PMMA standards at 40 °C in THF. [c] The target number average molecular weight. [d] The reaction time (minutes). [e] Z-average particle size (nm). [f] Molar fraction of IBOMA in Poly(C13MA-*grad*-IBOMA) determined by ^{1}H NMR in CDCl$_3$. [g] T$_m$ (melting point) and T$_g$ (glass transition temperature) measured by DSC under nitrogen atmosphere using three scans per cycle (heat/cool/heat) at a heating rate of 15 °C min^{-1} and cooling rate of 50 °C min^{-1}. [h] T$_{dec,1}$ (T$_{10\%}$ or onset of decomposition), T$_{dec,max}$ (temperature at which highest weight loss occurs) and T$_{dec,2}$ (end of decomposition) measured by TGA under nitrogen atmosphere at a ramp rate of 15 °C min^{-1}.

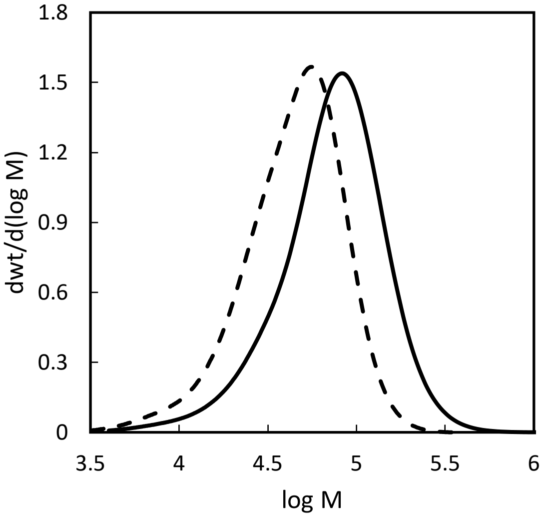

Figure 8. Molecular weight distribution of polymer particles in chain extension polymerization. Seed latex of poly(C13MA) (dashed black line) and poly(C13MA-*grad*-IBOMA) after the chain extension (solid black line). Characterization data for these two samples is provided in Table 6.

To evaluate the thermal stability and find the glass transition temperatures of poly(C13MA-*grad*-IBOMA), TGA and DSC were performed. The decomposition temperatures and glass transition temperatures are presented in Table 6(C). The first glass transition temperature (T$_{g,1}$) and melting temperature (T$_m$) corresponds to the soft C13MA block and the higher glass transition temperature

($T_{g,2}$) corresponds to the block of IBOMA-rich composition. The C13MA monomer used in this study is a mixture of methacrylic esters with an average chain length of 13 units. This results in the presence of monomers such as dodecyl methacrylate, tetradecyl methacrylate and other long chain monomers that produce homopolymers with semi-crystalline structures and melting points (e.g. T_ms for poly(dodecyl methacrylate) and poly(tetradecyl methacrylate) are -34 °C and -2 °C respectively)[91, 128, 129]. The inclusion of these monomers in C13MA likely cause the appearance of melting for the poly(C13MA-*grad*-IBOMA). Note that the higher T_g corresponding to the IBOMA-rich segment is lower than the T_g of poly(IBOMA) homopolymer from literature ($T_g \approx 110\sim200$ °C)[91-94] since there is likely some C13MA copolymerized in the former, resulting in a depression of the T_g. Still, the presence of multiple T_gs show the gradient polymerization of C13MA and IBOMA was sufficiently effective in producing compositionally distinctive blocks long enough to result in microphase separation[128]. The DSC trace for poly(C13MA-*grad*-IBOMA) is depicted in Figure S5 (see Supplementary Information).

Thermal Studies of IBOMA/C13MA Polymers Prepared in Solution and Emulsion Systems

TGA was performed for copolymers with different ratios of IBOMA/C13MA monomers to measure the decomposition temperatures of samples. The decomposition temperatures for two different systems were given in Table 7. The TGA results for copolymers with a high concentration of IBOMA monomers (initial IBOMA mol% > 30 %) show a two stage decomposition. This suggests the cleavage of the O-isobornyl bond and the formation of camphene in the sample and the elimination of it at higher temperatures[130]. This result was observed in other studies for copolymers containing IBOMA [83, 117]. Therefore, it can be concluded that polymers containing high concentrations of IBOMA will decompose readily and this may limit their applications at higher temperatures, although the polymers have a high T_g. The T_g and T_m were also measured by

DSC and the results are available in Table 7. The Fox equation was used to calculate the theoretical T_g for the resins[131]. For a polymer consisting of a mixture of different monomers, $T_{g,theo}$ can be estimated from the following equation:

$$\sum_i w_i \left(1 - \frac{T_{g,theo}}{T_{g,i}}\right) = 0 \tag{4}$$

where w_i is mass fraction of component i in polymer resin, $T_{g,theo}$ is the theoretical glass transition temperature of the resin and $T_{g,i}$ is the glass transition temperature of pure homopolymer of component i. $T_{g,IBOMA}$ and $T_{g,C13MA}$ were chosen from the experimental data presented in this study for each system. The resulting $T_{g,theo}$s for polymers with different ratio of IBOMA and C13MA monomers are listed in Table 7.

DSC indicates a single T_g for each statistical copolymerization, which is evidence of a homogeneous single-phase polymer [132]. From these measurements, the T_g of the final copolymer resins was predictably enhanced by increasing the [IBOMA]/[C13MA] ratio due to the higher T_g of IBOMA-based resins[95, 96]. The molecular structure of IBOMA consists of a 6-membered ring, which improves the heat resistance of this monomer and the polymer resins consequently[89]. Poly(C13MA) resins have a T_m and a T_g in both systems which agrees with literature for poly(methacrylate)s with long linear aliphatic carbon chains[128, 133]. Figure 9 illustrates the $T_{g,theo}$s and T_gs of IBOMA/C13MA copolymers prepared in two different systems (solution and emulsion). The T_gs and T_ms for samples produced in emulsion are lower than those of samples synthesized in solution system. This likely shows the effects of the addition of n-hexadecane (costabilizer) and DOWFAX™ 8390 (surfactant) to the polymer latex, where they act as plasticizers [134-137]. Some n-hexadecane molecules may present after the precipitation of polymer samples in methanol as it is insoluble in methanol at room temperature[138]. As mentioned in the previous section, the existence of melting points for samples with high concentrations of C13MA in miniemulsion polymerization can be due to the presence of long chain methacrylic esters (e.g. C12MA or C14MA). However, the copolymers obtained from emulsions with higher concentrations of IBOMA monomers are amorphous and do not have melting points (see Figure S6 in Supplementary Information for lack of crystallinity in IBOMA-rich copolymers).

Table 7. Results for thermal characterization of IBOMA/C13MA copolymers made in homogeneous organic solvent solution and emulsion systems

Solution system (polymers made in 50 wt% toluene)

Experiment ID	T_m^{a} (°C)	T_g^{a} (°C)	$T_{g,theo}$^{b} (°C)	$T_{dec,1}$^{c} (°C)	$T_{dec,max}$^{c}(°C)	$T_{dec,2}$^{c} (°C)	F_{IBOMA}^{d}	M_n^{e} (kg mol^{-1})
IBOMA100-S-100C	-	169	169	278	339	478	1	16.5
C13MA100-S-110C	-18	-31	-31	221	306	463	0	20.0
IBOMA80/C13MA20-S	-	69	98	232	317	476	0.80	23.6
IBOMA60/C13MA40-S	-	33	50	215	336	472	0.58	25.0
IBOMA50/C13MA50-S	-	12	31	225	314	476	0.48	26.1
IBOMA40/C13MA60-S	-	15	15	217	308	478	0.32	24.1
IBOMA30/C13MA70-S	-	2	2	186	291	461	0.24	26.5
IBOMA20/C13MA80-S	-	-10	-11	227	308	473	0.18	27.3
IBOMA10/C13MA90-S	-	-40	-21	203	295	450	0.06	19.8

Emulsion system

Experiment ID	T_m (°C)	T_g (°C)	$T_{g,theo}$ (°C)	$T_{dec,1}$ (°C)	$T_{dec,max}$ (°C)	$T_{dec,2}$ (°C)	F_{IBOMA}	M_n (kg mol^{-1})
IBOMA100	-	110	110	240	307	466	1	42.2
IBOMA100-83C	-	123	-	195	320	472	1	39.3
IBOMA100-100C	-	117	-	208	311	480	1	33.5
IBOMA90/C13MA10	-	81	82	235	323	470	0.9	53.9
IBOMA80/C13MA20	-	33	58	208	324	464	0.78	57.8
IBOMA70/C13MA30	-	30	39	216	335	486	0.68	46.8
IBOMA60/C13MA40	-	18	22	206	337	470	0.59	56.2
IBOMA50/C13MA50	-	-10	7	211	309	482	0.52	50.8
IBOMA40/C13MA60	-	-18	-6	224	310	501	0.38	64.2
IBOMA30/C13MA70	-	-17	-17	207	313	469	0.29	67.9
IBOMA20/C13MA80	-33	-52	-27	217	305	503	0.18	63.8
IBOMA10/C13MA90	-26	-42	-36	223	290	466	0.10	61.1
C13MA100	-19	-44	-44	174	296	468	0	48.9

[a] T_m (melting point) and T_g (glass transition temperature) measured by DSC under nitrogen atmosphere using three scans per cycle (heat/cool/heat) at a heating rate of 15 °C min^{-1} and cooling rate of 50 °C min^{-1}. [b] Theoretical glass transition temperature predicted by Fox equation. [c] $T_{dec,1}$ ($T_{10\%}$ or onset of decomposition), $T_{dec,max}$ (temperature at which highest weight loss occurs) and $T_{dec,2}$ (end of decomposition) measured by TGA under nitrogen atmosphere at a ramp rate of 15 °C min^{-1}. [d] Molar fraction of IBOMA in copolymers determined by ^{1}H NMR in $CDCl_3$. [e] The final number average molecular weight (M_n) was estimated using GPC with PMMA standards at 40 °C in THF.

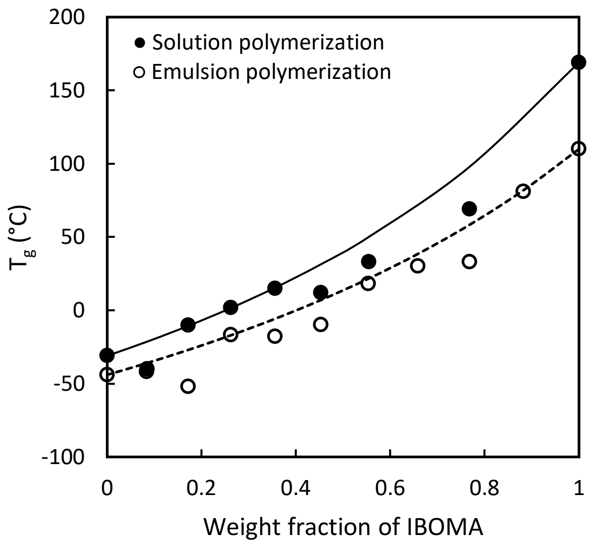

Figure 9. Evolution of T_g with weight fraction of IBOMA. The solid black line represents the $T_{g,theo}$ of copolymers synthesized in organic solvent as calculated by the Fox equation using the homopolymers made in solution as endpoints. The black dotted line shows the $T_{g,theo}$ for the emulsion system using homopolymers made in emulsion as endpoints. The black filled circles depict the experimental T_g for IBOMA/C13MA copolymers synthesized in 50 wt% toluene. The open circles represent the experimental T_g for IBOMA/C13MA copolymers with different weight fraction of IBOMA synthesized in emulsion.

Tensile Results for Poly(IBOMA-*b*-C13MA) and Poly(C13MA-*grad*-IBOMA)

To study the effect of the C13MA block on the mechanical properties of the copolymers, tensile tests were conducted on gradient and block copolymers prepared in emulsion and solution (toluene as the solvent), respectively, to illustrate the range of possible tensile properties. Figure 10 illustrated the stress-strain curves for Poly(IBOMA-*b*-C13MA) (F_{IBOMA} = 0.22, M_n = 37.1 kg mol^{-1}, Đ = 1.93) and poly(C13MA-*grad*-IBOMA) (F_{IBOMA} = 0.51, M_n = 54.0 kg mol^{-1}, Đ = 1.65) samples at room temperature. The strain at break for poly(C13MA-*grad*-IBOMA) sample made from miniemulsion polymerization was significantly lower than the poly(IBOMA-*b*-C13MA) sample (1.5% compared to 201%) due to the higher fraction of stiff IBOMA units incorporated in the copolymer. This agrees with the thermal results where increasing IBOMA incorporation into the copolymer increased the T_g of copolymers and subsequently made it more brittle. The linear elastic region for poly(IBOMA-*b*-C13MA) remained until 61.7% elongation and the yield strength of 0.77 MPa was achieved. The semi-plateau region (approximately 60-200% elongation) corresponds to plastic behavior of the block copolymer before finally breaking, which suggests that C13MA block can act as a plasticizer in poly(IBOMA-*b*-C13MA). These two IBOMA/C13MA copolymer examples show how mechanical properties are readily altered by simply applying different polymerization protocols and feed compositions.

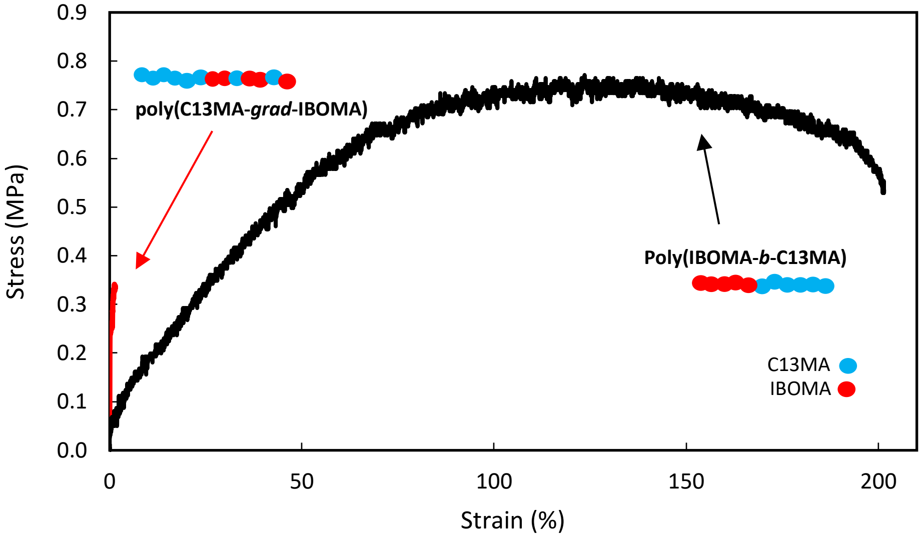

Figure 10. Stress-strain curves for poly(IBOMA-*b*-C13MA) (F_{IBOMA} = 0.22) and poly(C13MA-*grad*-IBOMA) (F_{IBOMA} = 0.51) samples at room temperature.

Rheological Measurements

The effect of monomer blocks and their compositions on rheological behavior of the resulting copolymers was done using the same copolymers in the section above (poly(IBOMA-*b*-C13MA) ($F_{\mathrm{IBOMA}} = 0.22$, prepared in toluene) and poly(C13MA-*grad*-IBOMA) ($F_{\mathrm{IBOMA}} = 0.51$, prepared in emulsion)) (Figure 11). Additionally, IBOMA20/C13MA80, IBOMA50/C13MA50 and IBOMA80/C13MA20 statistical copolymers prepared by miniemulsion NMP were also examined (Figure S7, Supplementary Information). All the samples from the emulsion system were dried and precipitated in methanol and dried again before the test. Figure 11 shows the dependence of storage modulus (G') and loss modulus (G") on frequency for poly(IBOMA-*b*-C13MA) and poly(C13MA-*grad*-IBOMA) at 140 ºC. The frequency sweep was performed in the range of 1-1000 Hz and the temperature of 140 ºC was chosen as all the polymer samples were in the melt state and $T > T_g$. This temperature can be used as an initial point to process the copolymers in the melt. The results at different temperatures were presented in Supplementary Information (Figure S8). G" for poly(C13MA-*grad*-IBOMA) was always higher than G', suggesting a viscous liquid behavior for the resins at all considered frequencies, with no cross-over observed. Similar behaviour was reported by Larson et al[139] for poly(styrene)-block-poly(isoprene) (PS-PI) diblock copolymer below the order-disorder transition temperature (T_{ODT}). At lower frequencies ($\omega < 250$ Hz), poly(IBOMA-*b*-C13MA) shows viscoelastic solid behavior with G´ dominating. A transition region was observed at high frequencies due to relaxation and dissipation mechanisms[140-143]. During this period, the G" increases faster than G', which resulted in a crossover (where G' = G") at 250 Hz. At frequencies higher than 250 Hz, a glassy region was observed, where G" is higher and increases more sharply in comparison to G'. Based on these results, the presence of the block of poly(C13MA) imparted more rubbery character into the final block copolymer, as expected.

This also was shown in the stress-strain curves for the same samples. The viscoelastic behaviour exhibited by the block copolymer was not observed for IBOMA/C13MA copolymers prepared via statistical copolymerization. The storage modulus (G') and loss modulus (G") versus frequency at 140 °C for 3 statistical copolymers with different compositions and prepared in emulsion were depicted in Figure S7 (Supplementary Information). In all the samples G" > G' at frequencies higher than 0.5 Hz, indicating primarily viscous behaviour. Thus, only in the case for the poly(IBOMA-*b*-C13MA) was primarily elastic behavior observed. This was not the case for statistical or gradient polymers even with a high C13MA fraction (compared with the results on Figure S8 in Supplementary Information) which suggests that the microstructure influenced the relaxation spectra of the material. To support the elastic behaviour of IBOMA/C13MA block copolymer, the Flory-Huggins interaction parameter χ[144] for the IBOMA/C13MA system was estimated to be 0.012 at 140 °C which suggests a partially miscible system for IBOMA/C13MA monomers (Supplementary Information Section 9). At the ODT, $\chi N \approx 10.5$ and our cN < 10.5 which suggests our block copolymers are in a disordered state[145].

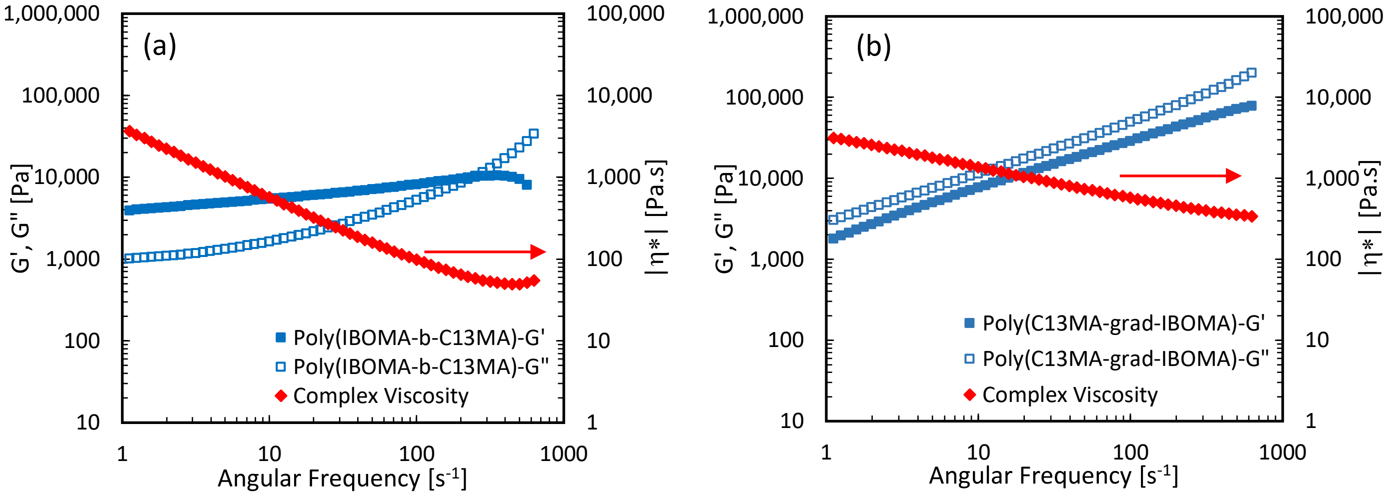

Figure 11. G', G" and complex viscosity plots versus shearing frequency for (a) Poly(IBOMA-*b*-C13MA) and (b) poly(C13MA-*grad*-IBOMA) polymers at 140 °C.

CONCLUSIONS

In this study, the copolymerization of commercially available bio-based methacrylic IBOMA and C13MA monomers was conducted in homogeneous toluene solution and then in a miniemulsion system by nitroxide mediated polymerization without any controlling comonomer. The reaction temperature for having a controlled polymerization of IBOMA/C13MA in emulsion was 90°C, which was 10 °C lower than the same system in organic solvent. Copolymers with different IBOMA:C13MA composition were synthesized in toluene (50 wt%) using Dispolreg 007 initiator. The slow initiation of Dispolreg 007 alkoxyamine was observed for the methacrylates and the early termination of macro-radicals occurred at higher conversions (X>50%) for NMP in toluene. However, the dispersity was relatively low ($1.39 < Đ < 1.66$) and polymer chains were able to be re-initiated to produce block copolymers. This system has two major drawbacks: using volatile organic solvent (toluene) and relatively lower monomer conversion caused by high viscosity. To overcome these problems, a miniemulsion polymerization technique was utilized to make the overall process greener and more efficient. The oil-soluble Dispolreg 007 was used as the initiator to start the polymerization within ~300-500 nm-sized monomer droplets. The monomer conversion reached as high as 94% while the dispersity was comparable to the toluene-based system ($1.50 < Đ < 1.73$) and the average final particle size of polymer particles was 270-550 nm. The final average molecular weight of polymers in solution (50 wt% in toluene) and emulsion was higher than the $M_{n,target}$, suggesting slow initiation of the Dispolreg 007 initiator for the polymerization of methacrylates. The ability to chain-extend the polymer resins prepared in emulsion was studied to verify the chain end fidelity and show that gradient or block copolymers are possible in the emulsion system. The thermal studies showed that the addition of IBOMA in the polymer resins increases the T_g relative to C13MA and readily allows the hardness or flexibility of the copolymers to be adjusted. Tensile tests showed that having about 80% C13MA resulted in high elongation at breaks ~ 200% and essentially elastic behavior. In the melt, the elastic modulus dominated in the block copolymer of IBOMA and C13MA always being higher than the viscous modulus in the frequency range studied, while the statistical and gradient polymers showed viscous liquid behavior.

ASSOCIATED CONTENT

Supporting Information

The Supplementary information consists of the following:

Composition of copolymers at the early stages of polymerization, Temperature studies in solution polymerization, Effect of feed composition on solution copolymerization by Dispolreg 007, Multiple Gaussian peak fitting for estimation of dead polymer chains in Poly(IBOMA)-*b*-poly(C13MA), Temperature studies in miniemulsion polymerization, Particle size in miniemulsion polymerization, DSC trace for poly(C13MA-*grad*-IBOMA) gradient copolymer, PXRD results, Rheological measurements, Flory-Huggins interaction parameter for Poly(IBOMA-*b*-C13MA). This information is available free of charge via the Internet at http://pubs.acs.org/.

AUTHOR INFORMATION

Corresponding Author

* milan.maric@mcgill.ca.

ORCID

Saeid Tajbakhsh: 0000-0003-4177-3272

Faezeh Hajiali: 0000-0003-1739-3966

Milan Marić: 0000-0002-4984-8761

Notes

The authors declare no competing financial interest.

ACKNOWLEDGMENT

McGill Engineering Doctoral Award (MEDA; McConnell Memorial) scholarship from the Faculty of Engineering, McGill University, Natural Sciences and Engineering Research Council (NSERC CRDPJ 518396-17 with Safran Cabin) and PRIMA Quebec with Safran Cabin (Project # R15-46-004) are gratefully acknowledged for their financial support. We also thank the Centre Québécois sur les Matériaux Fonctionnels (CQMF) for the use of the DSC and TGA.

REFERENCES

1. Grishin, D.; Grishin, I., Controlled radical polymerization: Prospects for application for industrial synthesis of polymers. *Russ. J. Appl. Chem.* **2011,** *84* (12), 2021-2028.
2. Destarac, M., Industrial development of reversible-deactivation radical polymerization: is the induction period over? *Polym. Chem.* **2018,** *9* (40), 4947-4967.
3. Matyjaszewski, K.; Spanswick, J., Controlled/living radical polymerization. *Mater. Today* **2005,** *8* (3), 26-33.
4. Braunecker, W. A.; Matyjaszewski, K., Controlled/living radical polymerization: Features, developments, and perspectives. *Prog. Polym. Sci.* **2007,** *32* (1), 93-146.
5. Destarac, M., Controlled radical polymerization: industrial stakes, obstacles and achievements. *Macromol. React. Eng.* **2010,** *4* (3-4), 165-179.
6. Nicolas, J.; Guillaneuf, Y.; Lefay, C.; Bertin, D.; Gigmes, D.; Charleux, B., Nitroxide-mediated polymerization. *Prog. Polym. Sci.* **2013,** *38* (1), 63-235.
7. Grubbs, R. B., Nitroxide-mediated radical polymerization: limitations and versatility. *Polym. Rev.* **2011,** *51* (2), 104-137.

8. Moad, G.; Rizzardo, E.; Thang, S. H., Living radical polymerization by the RAFT process–a second update. *Aust. J. Chem.* **2009,** *62* (11), 1402-1472.

9. Moad, G.; Barner-Kowollik, C., The Mechanism and Kinetics of the RAFT Process: Overview, Rates, Stabilities, Side Reactions, Product Spectrum and Outstanding Challenges. In *Handbook of RAFT Polymerization*, Barner-Kowollik, C., Ed. Wiley-VCH: Weinheim, 2008; pp 51-104.

10. Matyjaszewski, K.; Xia, J., Atom transfer radical polymerization. *Chem. Rev.* **2001,** *101* (9), 2921-2990.

11. di Lena, F.; Matyjaszewski, K., Transition metal catalysts for controlled radical polymerization. *Prog. Polym. Sci.* **2010,** *35* (8), 959-1021.

12. Mei, W.; Maric, M., Nitroxide-Mediated Polymerization of 2-Hydroxyethyl Methacrylate (HEMA) Controlled with Low Concentrations of Acrylonitrile and Styrene. *Macromol. React. Eng.* **2017,** *11* (3), 1600067.

13. Cunningham, M. F., Controlled/living radical polymerization in aqueous dispersed systems. *Prog. Polym. Sci.* **2008,** *33* (4), 365-398.

14. Cunningham, M. F., Living/controlled radical polymerizations in dispersed phase systems. *Prog. Polym. Sci.* **2002,** *27* (6), 1039-1067.

15. Monteiro, M. J.; Cunningham, M. F., Polymer Nanoparticles via Living Radical Polymerization in Aqueous Dispersions: Design and Applications. *Macromolecules* **2012,** *45* (12), 4939-4957.

16. Kobatake, S.; Harwood, H. J.; Quirk, R. P.; Priddy, D. B., Synthesis of Nitroxide-Functionalized Polybutadiene Using Halogen-Containing Benzyloxyamine as Terminators for Anionic Polymerization. *Macromolecules* **1999,** *32* (1), 10-13.

17. Percec, V.; Guliashvili, T.; Ladislaw, J. S.; Wistrand, A.; Stjerndahl, A.; Sienkowska, M. J.; Monteiro, M. J.; Sahoo, S., Ultrafast synthesis of ultrahigh molar mass polymers by metal-catalyzed living radical polymerization of acrylates, methacrylates, and vinyl chloride mediated by SET at 25 C. *J. Am. Chem. Soc.* **2006,** *128* (43), 14156-14165.

18. Fleischmann, S.; Rosen, B. M.; Percec, V., SET-LRP of acrylates in air. *J. Polym. Sci., Part A: Polym. Chem.* **2010,** *48* (5), 1190-1196.

19. Jakubowski, W.; Matyjaszewski, K., Activators Regenerated by Electron Transfer for Atom-Transfer Radical Polymerization of (Meth)acrylates and Related Block Copolymers. *Angew. Chem., Int. Ed.* **2006,** *45* (27), 4482-4486.

20. Jakubowski, W.; Min, K.; Matyjaszewski, K., Activators Regenerated by Electron Transfer for Atom Transfer Radical Polymerization of Styrene. *Macromolecules* **2006,** *39* (1), 39-45.

21. Engelis, N. G.; Anastasaki, A.; Nurumbetov, G.; Truong, N. P.; Nikolaou, V.; Shegiwal, A.; Whittaker, M. R.; Davis, T. P.; Haddleton, D. M., Sequence-controlled methacrylic multiblock copolymers via sulfur-free RAFT emulsion polymerization. *Nat. Chem.* **2017,** *9* (2), 171.

22. Zetterlund, P. B.; Yamazoe, H.; Yamada, B., Addition-Fragmentation Chain Transfer Involving Dimers of α-Methylvinyl Monomers Studied by ESR Spectroscopy: Competition between Fragmentation and Bimolecular Termination. *Macromol. Rapid Commun.* **2003,** *24* (2), 197-201.

23. Tian, X.; Ding, J.; Zhang, B.; Qiu, F.; Zhuang, X.; Chen, Y., Recent advances in RAFT polymerization: Novel initiation mechanisms and optoelectronic applications. *Polymers* **2018,** *10* (3), 318.

24. Treat, N. J.; Sprafke, H.; Kramer, J. W.; Clark, P. G.; Barton, B. E.; Read de Alaniz, J.; Fors, B. P.; Hawker, C. J., Metal-free atom transfer radical polymerization. *J. Am. Chem. Soc.* **2014,** *136* (45), 16096-16101.
25. Pearson, R. M.; Lim, C.-H.; McCarthy, B. G.; Musgrave, C. B.; Miyake, G. M., Organocatalyzed Atom Transfer Radical Polymerization Using N-Aryl Phenoxazines as Photoredox Catalysts. *J. Am. Chem. Soc.* **2016,** *138* (35), 11399-11407.
26. Wang, J.; Yuan, L.; Wang, Z.; Rahman, M. A.; Huang, Y.; Zhu, T.; Wang, R.; Cheng, J.; Wang, C.; Chu, F.; Tang, C., Photoinduced Metal-Free Atom Transfer Radical Polymerization of Biomass-Based Monomers. *Macromolecules* **2016,** *49* (20), 7709-7717.
27. Discekici, E. H.; Anastasaki, A.; Read de Alaniz, J.; Hawker, C. J., Evolution and Future Directions of Metal-Free Atom Transfer Radical Polymerization. *Macromolecules* **2018,** *51* (19), 7421-7434.
28. Gigmes, D., *Nitroxide Mediated Polymerization : From Fundamentals to Applications in Materials Science*. Royal Society of Chemistry: Croydon, 2015; pp 1-493.
29. Benoit, D.; Chaplinski, V.; Braslau, R.; Hawker, C. J., Development of a universal alkoxyamine for "living" free radical polymerizations. *J. Am. Chem. Soc.* **1999,** *121* (16), 3904-3920.
30. Hawker, C. J.; Bosman, A. W.; Harth, E., New polymer synthesis by nitroxide mediated living radical polymerizations. *Chem. Rev.* **2001,** *101* (12), 3661-3688.
31. Lessard, B.; Ling, E. J. Y.; Morin, M. S. T.; Marić, M., Nitroxide-mediated radical copolymerization of methyl methacrylate controlled with a minimal amount of 9-(4-vinylbenzyl)-9H-carbazole. *J. Polym. Sci., Part A: Polym. Chem.* **2011,** *49* (4), 1033-1045.
32. Marić, M.; Lessard, B. H.; Consolante, V.; Ling, E. J. Y., Incorporating primary amine pendant groups into copolymers via nitroxide mediated polymerization. *React. Funct. Polym.* **2011,** *71* (12), 1137-1147.
33. Ananchenko, G. S.; Souaille, M.; Fischer, H.; Le Mercier, C.; Tordo, P., Decomposition of model alkoxyamines in simple and polymerizing systems. II. Diastereomeric N-(2-methylpropyl)-N-(1-diethyl-phosphono-2, 2-dimethyl-propyl)-aminoxyl-based compounds. *J. Polym. Sci., Part A: Polym. Chem.* **2002,** *40* (19), 3264-3283.
34. Dire, C.; Belleney, J.; Nicolas, J.; Bertin, D.; Magnet, S.; Charleux, B., β-Hydrogen transfer from poly (methyl methacrylate) propagating radicals to the nitroxide SG1: Analysis of the chain-end and determination of the rate constant. *J. Polym. Sci., Part A: Polym. Chem.* **2008,** *46* (18), 6333-6345.
35. Greene, A. C.; Grubbs, R. B., Nitroxide-Mediated Polymerization of Methyl Methacrylate and Styrene with New Alkoxyamines from 4-Nitrophenyl 2-Methylpropionat-2-yl Radicals. *Macromolecules* **2010,** *43* (24), 10320-10325.
36. Charleux, B.; Nicolas, J.; Guerret, O., Theoretical Expression of the Average Activation−Deactivation Equilibrium Constant in Controlled/Living Free-Radical Copolymerization Operating via Reversible Termination. Application to a Strongly Improved Control in Nitroxide-Mediated Polymerization of Methyl Methacrylate. *Macromolecules* **2005,** *38* (13), 5485-5492.
37. Darabi, A.; Cunningham, M. F., Preparation of Poly (poly (ethylene glycol) methyl ether methacrylate-co-styrene)-b-poly (2-(diethylamino) ethyl methacrylate-co-acrylonitrile) by nitroxide-mediated polymerisation in water. *Polymer* **2017,** *115*, 255-260.
38. Darabi, A.; Shirin-Abadi, A. R.; Jessop, P. G.; Cunningham, M. F., Nitroxide-mediated polymerization of 2-(diethylamino) ethyl methacrylate (DEAEMA) in water. *Macromolecules* **2014,** *48* (1), 72-80.

39. Nicolas, J.; Brusseau, S.; Charleux, B., A minimal amount of acrylonitrile turns the nitroxide-mediated polymerization of methyl methacrylate into an almost ideal controlled/living system. *J. Polym. Sci., Part A: Polym. Chem.* **2010,** *48* (1), 34-47.

40. Lessard, B.; Ling, E. J. Y.; Morin, M. S. T.; Marić, M., Nitroxide-mediated radical copolymerization of methyl methacrylate controlled with a minimal amount of 9-(4-vinylbenzyl)-9H-carbazole. *J. Polym. Sci., Part A: Polym. Chem.* **2011,** *49* (4), 1033-1045.

41. Lessard, B. H.; Guillaneuf, Y.; Mathew, M.; Liang, K.; Clement, J.-L.; Gigmes, D.; Hutchinson, R. A.; Marić, M., Understanding the controlled polymerization of Methyl Methacrylate with low concentrations of 9-(4-Vinylbenzyl)-9 H-carbazole comonomer by nitroxide-mediated polymerization: The pivotal role of reactivity ratios. *Macromolecules* **2013,** *46* (3), 805-813.

42. Consolante, V.; Marić, M., Nitroxide-Mediated Polymerization of an Organo-Soluble Protected Styrene Sulfonate: Development of Homo-and Random Copolymers. *Macromol. React. Eng.* **2011,** *5* (11-12), 575-586.

43. Brusseau, S.; Belleney, J.; Magnet, S.; Couvreur, L.; Charleux, B., Nitroxide-mediated copolymerization of methacrylic acid with sodium 4-styrene sulfonate: Towards new water-soluble macroalkoxyamines for the synthesis of amphiphilic block copolymers and nanoparticles. *Polym. Chem.* **2010,** *1* (5), 720-729.

44. Darabi, A.; García-Valdez, O.; Champagne, P.; Cunningham, M. F., PEGylation of Chitosan Via Nitroxide-Mediated Polymerization in Aqueous Media. *Macromol. React. Eng.* **2016,** *10* (1), 82-89.

45. Greene, A. C.; Grubbs, R. B., Nitroxide-Mediated Polymerization of Methyl Methacrylate and Styrene with New Alkoxyamines from 4-Nitrophenyl 2-Methylpropionat-2-yl Radicals. *Macromolecules* **2010,** *43*, 10320.

46. Detrembleur, C.; Teyssié, P.; Jérôme, R., Control of the Radical Polymerization of tert-Butyl Methacrylate in Water by a Novel Combination of Sodium Nitrite and Iron(II) Sulfate. *Macromolecules* **2002,** *35* (5), 1611-1621.

47. Guillaneuf, Y.; Gigmes, D.; Marque, S. R.; Astolfi, P.; Greci, L.; Tordo, P.; Bertin, D., First effective nitroxide-mediated polymerization of methyl methacrylate. *Macromolecules* **2007,** *40* (9), 3108-3114.

48. Ballard, N.; Aguirre, M.; Simula, A.; Agirre, A.; Leiza, J. R.; Asua, J. M.; van Es, S., New Class of Alkoxyamines for Efficient Controlled Homopolymerization of Methacrylates. *ACS Macro Lett.* **2016,** *5* (9), 1019-1022.

49. Simula, A.; Aguirre, M.; Ballard, N.; Veloso, A.; Leiza, J. R.; van Es, S.; Asua, J. M., Novel alkoxyamines for the successful controlled polymerization of styrene and methacrylates. *Polym. Chem.* **2017,** *8* (10), 1728-1736.

50. Simula, A.; Ruipérez, F.; Ballard, N.; Leiza, J. R.; van Es, S.; Asua, J. M., Why can Dispolreg 007 control the nitroxide mediated polymerization of methacrylates? *Polym. Chem.* **2019,** *10* (1), 106-113.

51. Marestin, C.; Noël, C.; Guyot, A.; Claverie, J., Nitroxide mediated living radical polymerization of styrene in emulsion. *Macromolecules* **1998,** *31* (12), 4041-4044.

52. Porzio, R. S.; Zhao, C.-L.; Anchor, M. J. Low-VOC emulsion polymer coating compositions. U.S. Patent 7,705,081, Apr. 27, 2010.

53. Batlaw, R.; Moore, P. D. Printing ink emulsion having reduced VOC. U.S. Patent 5,389,130, Feb. 14, 1995.

54. Ballard, N.; Aguirre, M.; Simula, A.; Leiza, J. R.; van Es, S.; Asua, J. M., Nitroxide mediated suspension polymerization of methacrylic monomers. *Chem. Eng. J.* **2017,** *316* (Supplement C), 655-662.

55. Cao, J.; He, J.; Li, C.; Yang, Y., Nitroxide-mediated radical polymerization of styrene in emulsion. *Polym. J.* **2001,** *33* (1), 75-80.

56. Nicolas, J.; Charleux, B.; Guerret, O.; Magnet, S., Nitroxide-Mediated Controlled Free-Radical Emulsion Polymerization Using a Difunctional Water-Soluble Alkoxyamine Initiator. Toward the Control of Particle Size, Particle Size Distribution, and the Synthesis of Triblock Copolymers. *Macromolecules* **2005,** *38* (24), 9963-9973.

57. Groison, E.; Brusseau, S.; D'Agosto, F.; Magnet, S.; Inoubli, R.; Couvreur, L.; Charleux, B., Well-Defined Amphiphilic Block Copolymer Nanoobjects via Nitroxide-Mediated Emulsion Polymerization. *ACS Macro Lett.* **2012,** *1* (1), 47-51.

58. Ballard, N.; Aguirre, M.; Simula, A.; Leiza, J. R.; van Es, S.; Asua, J. M., High solids content nitroxide mediated miniemulsion polymerization of n-butyl methacrylate. *Polym. Chem.* **2017,** *8* (10), 1628-1635.

59. Guo, Y.; Zetterlund, P. B., Synthesis of nanosized (< 20 nm) polymer particles by radical polymerization in miniemulsion employing in situ surfactant formation. *Macromol. Rapid Commun.* **2011,** *32* (20), 1669-1675.

60. Mehravar, E.; Agirre, A.; Ballard, N.; van Es, S.; Arbe, A.; Leiza, J. R.; Asua, J. M., Insights into the Network Structure of Cross-Linked Polymers Synthesized via Miniemulsion Nitroxide-Mediated Radical Polymerization. *Macromolecules* **2018,** *51* (23), 9740-9748.

61. Li, W. S. J.; Cunningham, M. F., Nitroxide-mediated microemulsion polymerization of n-butyl acrylate: decoupling of target molecular weight and particle size. *Polym. Chem.* **2014,** *5* (12), 3804.

62. Zetterlund, P. B.; Wakamatsu, J.; Okubo, M., Nitroxide-mediated radical polymerization of styrene in aqueous microemulsion: Initiator efficiency, compartmentalization, and nitroxide phase transfer. *Macromolecules* **2009,** *42* (18), 6944-6952.

63. Brooks, B., Suspension polymerization processes. *Chemical Engineering & Technology* **2010,** *33* (11), 1737-1744.

64. Zetterlund, P. B., Controlled/living radical polymerization in nanoreactors: compartmentalization effects. *Polym. Chem.* **2011,** *2* (3), 534-549.

65. Qiu, J.; Charleux, B.; Matyjaszewski, K., Controlled/living radical polymerization in aqueous media: homogeneous and heterogeneous systems. *Prog. Polym. Sci.* **2001,** *26* (10), 2083-2134.

66. Rempel, G. L.; Wang, H., Microemulsion Polymerization. In *Encyclopedia of Polymeric Nanomaterials*, Kobayashi, S.; Müllen, K., Eds. Springer: Berlin, Heidelberg, 2015; pp 1241-1250.

67. Yong, C. P.; Gan, L. M., Microemulsion polymerizations and reactions. In *Polymer Particles*, Okubo, M., Ed. Springer: Berlin, Heidelberg, 2005; pp 257-298.

68. Monteiro, M. J., Nanoreactors for polymerizations and organic reactions. *Macromolecules* **2010,** *43* (3), 1159-1168.

69. Schork, F. J.; Luo, Y.; Smulders, W.; Russum, J. P.; Butté, A.; Fontenot, K., Miniemulsion Polymerization. In *Polymer Particles*, Okubo, M., Ed. Springer: Berlin, Heidelberg, 2005; pp 129-255.

70. Landfester, K., Miniemulsions for Nanoparticle Synthesis. In *Colloid Chemistry II*, Antonietti, M., Ed. Springer: Berlin, Heidelberg, 2003; pp 75-123.

71. Asua, J. M., Challenges for industrialization of miniemulsion polymerization. *Prog. Polym. Sci.* **2014,** *39* (10), 1797-1826.
72. Zetterlund, P. B.; Okubo, M., Compartmentalization in nitroxide-mediated radical polymerization in dispersed systems. *Macromolecules* **2006,** *39* (26), 8959-8967.
73. Zetterlund, P. B.; Thickett, S. C.; Perrier, S.; Bourgeat-Lami, E.; Lansalot, M., Controlled/Living Radical Polymerization in Dispersed Systems: An Update. *Chem. Rev.* **2015,** *115* (18), 9745-9800.
74. Asua, J. M., Miniemulsion polymerization. *Prog. Polym. Sci.* **2002,** *27* (7), 1283-1346.
75. Guo, Y.; Liu, J.; Zetterlund, P. B., Nitroxide-mediated radical polymerization in miniemulsion on the basis of in situ surfactant formation without use of homogenization device. *Macromolecules* **2010,** *43* (14), 5914-5916.
76. Alduncin, J. A.; Forcada, J.; Asua, J. M., Miniemulsion polymerization using oil-soluble initiators. *Macromolecules* **1994,** *27* (8), 2256-2261.
77. Molina-Gutiérrez, S.; Ladmiral, V.; Bongiovanni, R.; Caillol, S.; Lacroix-Desmazes, P., Radical polymerization of biobased monomers in aqueous dispersed media. *Green Chem.* **2019,** *21* (1), 36-53.
78. Zhu, Y.; Romain, C.; Williams, C. K., Sustainable polymers from renewable resources. *Nature* **2016,** *540*, 354-362.
79. Meek, K. M.; Eaton, T. R.; Rorrer, N. A.; Brandner, D. G.; Manker, L. P.; Karp, E. M.; Biddy, M. J.; Bratis, A. D.; Beckham, G. T.; Naskar, A. K., Emulsion polymerization of acrylonitrile in aqueous methanol. *Green Chem.* **2018,** *20* (23), 5299-5310.
80. Semsarilar, M.; Perrier, S., 'Green' reversible addition-fragmentation chain-transfer (RAFT) polymerization. *Nat. Chem.* **2010,** *2*, 811-820.
81. Satoh, K., Controlled/living polymerization of renewable vinyl monomers into bio-based polymers. *Polym. J.* **2015,** *47*, 527-536.
82. Okada, S.; Matyjaszewski, K., Synthesis of bio-based poly(N-phenylitaconimide) by atom transfer radical polymerization. *J. Polym. Sci., Part A: Polym. Chem.* **2015,** *53* (6), 822-827.
83. Hajiali, F.; Métafiot, A.; Benitez-Ek, L.; Alloune, L.; Marić, M., Nitroxide mediated polymerization of sustainably sourced isobornyl methacrylate and tridecyl methacrylate with acrylonitrile co-monomer. *J. Polym. Sci., Part A: Polym. Chem.* **2018,** *56* (21), 2422-2436.
84. Qu, W.; Huang, Y.; Luo, Y.; Kalluru, S.; Cochran, E.; Forrester, M.; Bai, X., Controlled Radical Polymerization of Crude Lignin Bio-oil Containing Multihydroxyl Molecules for Methacrylate Polymers and the Potential Applications. *ACS Sustainable Chem. Eng.* **2019,** *7* (9), 9050-9060.
85. Hatton, F. L., Recent advances in RAFT polymerization of monomers derived from renewable resources. *Polym. Chem.* **2019,** *11* (2), 220-229.
86. Zheng, Y.; Yao, K.; Lee, J.; Chandler, D.; Wang, J.; Wang, C.; Chu, F.; Tang, C., Well-Defined Renewable Polymers Derived from Gum Rosin. *Macromolecules* **2010,** *43* (14), 5922-5924.
87. Noppalit, S.; Simula, A.; Billon, L.; Asua, J. M., On the nitroxide mediated polymerization of methacrylates derived from bio-sourced terpenes in miniemulsion, a step towards sustainable products. *Polym. Chem.* **2020,** *11* (6), 1151-1160.
88. Knebel, J.; Saal, D. Process for synthesis of isobornyl (Meth) acrylate. U.S. Patent 6,329,543, Dec. 11, 2001.
89. Chen, L.; Bao, Z.; Fu, Z.; Li, W., Preparation and characterisation of novel cross-linked poly (IBOMA-BA-DFMA) latex. *Pigment & Resin Technology* **2015,** *44* (6), 333-338.

90. Park, S. I.; Lee, S. I.; Hong, S.-J.; Cho, K. Y., Suspension polymerization and characterization of transparent poly(methyl methacrylate-co-isobornyl methacrylate). *Macromol. Res.* **2007,** *15* (5), 418-423.
91. Ellis, B.; Smith, R., *Polymers: a property database*. 2nd ed.; CRC Press: Boca Raton, 2008; pp 241-691.
92. Yu, J. M.; Dubois, P.; Jérôme, R., Synthesis and properties of poly [isobornyl methacrylate (IBMA)-b-butadiene (BD)-b-IBMA] copolymers: New thermoplastic elastomers of a large service temperature range. *Macromolecules* **1996,** *29* (23), 7316-7322.
93. Kaya, İ.; Özdemir, E., Thermodynamic interactions and characterisation of poly(isobornyl methacrylate) by inverse gas chromatography at various temperatures. *Polymer* **1999,** *40* (9), 2405-2410.
94. Kurt, A.; Kaya, E., Synthesis, characterization, and thermal degradation kinetics of the copolymer poly(4-methoxybenzyl methacrylate-co-isobornyl methacrylate). *J. Appl. Polym. Sci.* **2010,** *115* (4), 2359-2367.
95. Yu, J. M.; Dubois, P.; Jérôme, R., Synthesis and Properties of Poly[isobornyl methacrylate (IBMA)-b-butadiene (BD)-b-IBMA] Copolymers: New Thermoplastic Elastomers of a Large Service Temperature Range. *Macromolecules* **1996,** *29* (23), 7316-7322.
96. Zhang, B.; Ma, Y.; Chen, D.; Xu, J.; Yang, W., Preparation of poly(styrene-co-isobornyl methacrylate) beads having controlled glass transition temperature by suspension polymerization. *J. Appl. Polym. Sci.* **2013,** *129* (1), 113-120.
97. Meier, M. A. R.; Metzger, J. O.; Schubert, U. S., Plant oil renewable resources as green alternatives in polymer science. *Chem. Soc. Rev.* **2007,** *36* (11), 1788-1802.
98. Fenn, D. R.; Hughes, V. L. Coating compositions comprising isobornyl methacrylate and 4-hydroxybutyl acrylate. U.S. Patent 5,514,755, May 7, 1996.
99. Kitagawa, S.; Baba, M. Thermoplastic elastomer and a process for its production. U.S. Patent 5,183,856, Feb. 2, 1993.
100. Aoki, H.; Ito, M.; Miura, T.; Osuka, M. Thermoplastic resin composition and molded article comprising the same. U.S. Patent 7,589,151, Sep. 15, 2009.
101. Kawaguchi, Y.; Itamura, Y.; Onimura, K.; Oishi, T., Effects of the chemical structure on the heat resistance of thermoplastic expandable microspheres. *J. Appl. Polym. Sci.* **2005,** *96* (4), 1306-1312.
102. Qi, G.; Nolan, M.; Schork, F. J.; Jones, C. W., Emulsion and controlled miniemulsion polymerization of the renewable monomer γ-methyl-α-methylene-γ-butyrolactone. *J. Polym. Sci., Part A: Polym. Chem.* **2008,** *46* (17), 5929-5944.
103. ASTM D638-14, Standard Test Method for Tensile Properties of Plastics. ASTM International, West Conshohocken, PA, 2014.
104. Sabatini, D. A.; Harwell, J. H.; Hasegawa, M.; Knox, R., Membrane processes and surfactant-enhanced subsurface remediation: results of a field demonstration. *J. Membr. Sci.* **1998,** *151* (1), 87-98.
105. Hitchens, L.; Vane, L. M.; Alvarez, F. R., VOC removal from water and surfactant solutions by pervaporation: a pilot study. *Sep. Purif. Technol.* **2001,** *24* (1-2), 67-84.
106. Lee, D.-H.; Cody, R. D.; Kim, D.-J., Surfactant recycling by solvent extraction in surfactant-aided remediation. *Sep. Purif. Technol.* **2002,** *27* (1), 77-82.
107. Farcet, C.; Charleux, B.; Pirri, R., Poly(n-butyl acrylate) Homopolymer and Poly[n-butyl acrylate-b-(n-butyl acrylate-co-styrene)] Block Copolymer Prepared via Nitroxide-Mediated

Living/Controlled Radical Polymerization in Miniemulsion. *Macromolecules* **2001,** *34* (12), 3823-3826.

108. Babu, K. N.; Divakaran, M.; Ravindran, P.; Peter, K., Long pepper. In *Handbook of Herbs and Spices*, Peter, K. V., Ed. Woodhead Publishing: Cambridge, 2006; pp 420-437.

109. Callaghan, A. V.; Tierney, M.; Phelps, C. D.; Young, L. Y., Anaerobic biodegradation of n-hexadecane by a nitrate-reducing consortium. *Appl. Environ. Microbiol* **2009,** *75* (5), 1339-1344.

110. Simula, A.; Ballard, N.; Aguirre, M.; Leiza, J. R.; Es, S. v.; Asua, J. M., Nitroxide mediated copolymerization of acrylates, methacrylates and styrene: The importance of side reactions in the polymerization of acrylates. *Eur. Polym. J.* **2019,** *110*, 319-329.

111. Tidwell, P. W.; Mortimer, G. A., An improved method of calculating copolymerization reactivity ratios. *J. Polym. Sci., Part A: Gen. Pap.* **1965,** *3* (1), 369-387.

112. Odian, G., *Principles of Polymerization*. 4th ed.; John Wiley & Sons: Hoboken, 2004; pp 1-812.

113. Mayo, F. R.; Lewis, F. M., Copolymerization. I. A Basis for Comparing the Behavior of Monomers in Copolymerization; The Copolymerization of Styrene and Methyl Methacrylate. *J. Am. Chem. Soc.* **1944,** *66* (9), 1594-1601.

114. Stahl, G. A., Copolymerization of methyl methacrylate and dodecyl methacrylate. *J. Polym. Sci., Polym. Chem. Ed.* **1979,** *17* (6), 1883-1886.

115. Šoljić, I.; Jukić, A.; Janović, Z., Terpolymerization kinetics of N,N-dimethylaminoethyl methacrylate/alkyl methacrylate/styrene systems. *Polym. Eng. Sci.* **2010,** *50* (3), 577-584.

116. Rajdeo, K. S.; Ponrathnam, S.; Pardeshi, S.; Chavan, N. N.; Bhongale, S. S.; Harikrishna, R., Ambient Temperature Photocopolymerization of Tetrahydrofurfuryl Methacrylate and Isobornyl Methacrylate: Reactivity Ratios and Thermal Studies. *J. Macromol. Sci., Part A* **2015,** *52* (12), 982-991.

117. Kaya, E., Copolymers of 4-methoxybenzyl methacrylate and isobornyl methacrylate: synthesis, characterization and determination of monomer reactivity ratios. *J. Chem. Soc. Pak.* **2011,** *33*, 555-561.

118. Farcet, C.; Charleux, B.; Pirri, R., Nitroxide-mediated miniemulsion polymerization of n-butyl acrylate: synthesis of controlled homopolymers and gradient copolymers with styrene. *Macromol. Symp.* **2002,** *182* (1), 249-260.

119. Makati, A. C.; Kan, C. S.; Iwamasa, R. T.; Lee, D. I. Polymeric adhesion promoter and latexes; and polymeric adhesion promoter, epoxy resins and latexes are used to improve adherence between various substrates. U.S. Patent 5,569,686, Oct. 29, 1996.

120. Ivanković, T.; Hrenović, J., Surfactants in the environment. *Arch. Ind. Hyg. Toxicol.* **2010,** *61* (1), 95-110.

121. Cserháti, T.; Forgács, E.; Oros, G., Biological activity and environmental impact of anionic surfactants. *Environment International* **2002,** *28* (5), 337-348.

122. Önder, E.; Koparal, A. S.; Öğütveren, Ü. B., An alternative method for the removal of surfactants from water: Electrochemical coagulation. *Sep. Purif. Technol.* **2007,** *52* (3), 527-532.

123. Yuan, C.; Xu, Z.; Fan, M.; Liu, H.; Xie, Y.; Zhu, T., Study on characteristics and harm of surfactants. *J. Chem. Pharm. Res.* **2014,** *6* (7), 2233-2237.

124. Guillaneuf, Y.; Gigmes, D.; Marque, S. R. A.; Tordo, P.; Bertin, D., Nitroxide-Mediated Polymerization of Methyl Methacrylate Using an SG1-Based Alkoxyamine: How the Penultimate Effect Could Lead to Uncontrolled and Unliving Polymerization. *Macromol. Chem. Phys.* **2006,** *207* (14), 1278-1288.

125. Chern, C.-S.; Liou, Y.-C., Kinetics of styrene miniemulsion polymerization stabilized by nonionic surfactant/alkyl methacrylate. *Polymer* **1999,** *40* (13), 3763-3772.
126. Chern, C. S.; Chen, T. J., Miniemulsion polymerization of styrene using alkyl methacrylates as the reactive cosurfactant. *Colloid Polym. Sci.* **1997,** *275* (6), 546-554.
127. Chern, C.-S.; Liou, Y.-C., Effects of mixed surfactants on the styrene miniemulsion polymerization in the presence of an alkyl methacrylate. *Macromol. Chem. Phys.* **1998,** *199* (9), 2051-2061.
128. Fleischhaker, F.; Haehnel, A. P.; Misske, A. M.; Blanchot, M.; Haremza, S.; Barner-Kowollik, C., Glass-Transition-, Melting-, and Decomposition Temperatures of Tailored Polyacrylates and Polymethacrylates: General Trends and Structure–Property Relationships. *Macromol. Chem. Phys.* **2014,** *215* (12), 1192-1200.
129. Greenberg, S. A.; Alfrey, T., Side Chain Crystallization of n-Alkyl Polymethacrylates and Polyacrylates1. *J. Am. Chem. Soc.* **1954,** *76* (24), 6280-6285.
130. Matsumoto, A.; Mizuta, K.; Otsu, T., Synthesis and thermal properties of poly(cycloalkyl methacrylate)s bearing bridged- and fused-ring structures. *J. Polym. Sci., Part A: Polym. Chem.* **1993,** *31* (10), 2531-2539.
131. Fox, T. G., Influence of Diluent and Copolymer Composition on the Glass Temperature of a Polymer System. *Bull. Am. Phys. Soc* **1956,** *1*, 123.
132. Chen, L.; Jiang, W.; Wu, F., Nanometre fluorinated acrylate latex prepared with gemini surfactant. *Micro Nano Lett.* **2012,** *7* (8), 810-813.
133. Haehnel, A. P.; Schneider-Baumann, M.; Hiltebrandt, K. U.; Misske, A. M.; Barner-Kowollik, C., Global Trends for kp? Expanding the Frontier of Ester Side Chain Topography in Acrylates and Methacrylates. *Macromolecules* **2013,** *46* (1), 15-28.
134. Haq, Z.; Thompson, L., Significance of glass transition temperature to polymer latex stabilisation by nonionic surfactants. *Colloid Polym. Sci.* **1982,** *260* (2), 212-217.
135. Bouissou, C.; Rouse, J. J.; Price, R.; van der Walle, C. F., The Influence of Surfactant on PLGA Microsphere Glass Transition and Water Sorption: Remodeling the Surface Morphology to Attenuate the Burst Release. *Pharm. Res.* **2006,** *23* (6), 1295-1305.
136. McKinney, P. V., Processing of poly(vinyl chloride) polymers correlated with composition, glass transition, and viscosity. *J. Appl. Polym. Sci.* **1965,** *9* (10), 3359-3382.
137. Gruber, B. A.; Vratsanos, M. S.; Smith, C. D., Effects of colloidal stabilizer on vinyl acetate-ethylene copolymer emulsions and films. *Macromol. Symp.* **2000,** *155* (1), 163-170.
138. Rogalski, M.; Stryjek, R., Mutual solubility of binary n-hexadecane and polar compound systems. *Bull. Acad. Pol. Sci., Ser. Sci. Chim.* **1980,** *28* (2), 139-147.
139. Larson, R. G.; Winey, K. I.; Patel, S. S.; Watanabe, H.; Bruinsma, R., The rheology of layered liquids: lamellar block copolymers and smectic liquid crystals. *Rheol. Acta* **1993,** *32* (3), 245-253.
140. Barnes, H. A., *A Handbook of Elementary Rheology*. University of Wales, Institute of Non-Newtonian Fluid Mechanics: Aberystwyth, 2000; pp 81-106.
141. Vinogradov, G. V., Limiting regimes of deformation of polymers. *Polym. Eng. Sci.* **1981,** *21* (6), 339-351.
142. Borisenkova, E. K.; Dreval, V. E.; Vinogradov, G. V.; Kurbanaliev, M. K.; Moiseyev, V. V.; Shalganova, V. G., Transition of polymers from the fluid to the forced high-elastic and leathery states at temperatures above the glass transition temperature. *Polymer* **1982,** *23* (1), 91-99.

143. Vinogradov, G. V.; Dreval, V. Y.; Borisenkova, Y. K.; Kurbanaliyev, M. K.; Shalganova, V. G., Longitudinal deformation and rupture of linear flexible-chain polymers. *Polym. Sci. U.S.S.R.* **1981,** *23* (12), 2847-2860.
144. Flory, P. J., *Principles of Polymer Chemistry*. Cornell University Press: New York, 1953; pp 29-657.
145. Matsen, M. W.; Bates, F. S., Unifying Weak- and Strong-Segregation Block Copolymer Theories. *Macromolecules* **1996,** *29* (4), 1091-1098.

Graphical Abstract